

Unitary-invariant method for witnessing nonstabilizerness in quantum processors

Rafael Wagner^{1,2,3,4,10,*} , Filipa C R Peres^{1,5,6,10} , Emmanuel Zambrini Cruzeiro^{7,8} and Ernesto F Galvão^{1,9} 

¹ INL—International Iberian Nanotechnology Laboratory, Braga, Portugal

² Centro de Física, Universidade do Minho, Braga, Portugal

³ Department of Physics ‘E. Fermi’, University of Pisa, Pisa, Italy

⁴ Institute of Theoretical Physics, Ulm University, Albert-Einstein-Allee 11, 89081 Ulm, Germany

⁵ Departamento de Física e Astronomia, Faculdade de Ciências, Universidade do Porto, Porto, Portugal

⁶ Departamento de Electromagnetismo y Física de la Materia, Universidad de Granada, 18010 Granada, Spain

⁷ Departamento de Engenharia Electrotécnica e de Computadores, Instituto Superior Técnico, Lisbon, Portugal

⁸ Instituto de Telecomunicações, Lisbon, Portugal

⁹ Instituto de Física, Universidade Federal Fluminense, Niterói, RJ, Brazil

E-mail: rafael.wagner@uni-ulm.de

Received 28 April 2025; revised 1 June 2025

Accepted for publication 30 June 2025

Published 11 July 2025



Abstract

Nonstabilizerness, also known as ‘magic’, is a crucial resource for quantum computation. The growth in complexity of quantum processing units (QPUs) demands robust and scalable techniques for characterizing this resource. We introduce the basis-independent notion of *set magic*: a set of states has this property if at least one state in the set is a magic state. We show that certain two-state overlap inequalities, recently introduced as witnesses of basis-independent coherence, are also witnesses of set magic. Finally, we show that using such witnesses one can robustly certify nonstabilizerness in a network

¹⁰ These authors contributed equally.

* Author to whom any correspondence should be addressed.



Original Content from this work may be used under the terms of the [Creative Commons Attribution 4.0 licence](#). Any further distribution of this work must maintain attribution to the author(s) and the title of the work, journal citation and DOI.

of QPUs without having to entangle the different devices and with reduced demands compared to the individual certification of each QPU.

Keywords: nonstabilizerness, coherence witnesses, quantum processing unit, quantum resource certification

1. Introduction

The certification of quantum devices is a crucial task [1]. One fundamental characteristic of quantum computing hardware is the ability to generate non-classical resources: quantum coherence [2, 3], quantum entanglement [4, 5], Hilbert space dimension [6], quantum contextuality [7] are all necessary resources for quantum information processing. The growth in complexity of near-term noisy devices [8–10] demands *scalable* and *robust* methods for witnessing non-classical properties. This is something that has remained elusive for the case of nonstabilizerness [11], a resource without which quantum speed-up is impossible [12]. Nonstabilizerness fuels one of the main approaches to fault-tolerant quantum computation via the so-called magic-state injection scheme [11, 13] and is the most expensive resource to generate and characterize in some quantum computing architectures [11, 14–17].

In this work, we propose a technique for certifying the presence of nonstabilizerness in a network of quantum processing units (QPUs), without the need to entangle resources between separate units. Our protocol is efficient, robust, and based on estimating two-state overlaps $r_{i,j} = \text{Tr}(\rho_i \rho_j)$ (also known as fidelity, when one of the states is pure). An illustration of our test can be seen in figure 1. Interestingly, we can use this scheme to certify nonstabilizerness among various QPUs without having to entangle the different units. We envision many use cases. First, we can certify the presence of nonstabilizer resources in a single QPU. Secondly, we can certify the generation of nonstabilizerness by multiple QPUs in a network; for example, a referee collects overlap statistics from different QPUs and, after processing these values (i.e. calculating linear functionals of overlaps), they can infer that nonstabilizer resources were present in at least some QPUs. Moreover, our method can be used to certify (unknown) states shared by third parties and to detect nonstabilizerness present in n -qubit systems and not realizable by systems with fewer than n qubits. As such, we expect our results to be relevant both for the management of quantum networks—in the sense of certifying their correct operation and ability to generate nonstabilizer resources needed for quantum advantage—and for the delegated certification of quantum states [18, section 3.5].

Many tools for certifying nonstabilizerness exist. However, as the majority is aimed at the task of *resource quantification*—in the formal resource-theoretic sense [19]—rather than the simpler one of *witnessing*, most protocols have stringent requirements. Most commonly, there is a need for: (i) full tomographic information on the quantum states [20], (ii) purity of states (or restriction to specific subclasses of states) [21–23], (iii) additional entanglement generation [24, 25], or (iv) vertex characterization of the stabilizer polytope [26–30]. We avoid all of these requirements. Our certification scheme depends on two promises of the device-generated statistics: (a) the data is described by two-state overlaps and (b) the device consists of a multi-qubit system. For certain witnesses, it will be possible to relax the second requirement.

Our method is based on showing that some inequalities, initially introduced as coherence witnesses [31, 32], can also be used as witnesses of nonstabilizerness. The basis-independent nature of such inequalities implies the existence of a relational notion of nonstabilizerness defined for a set of states; we term this notion *set magic* or *set nonstabilizerness*. The idea of viewing set-based resources has recently emerged as a prominent research topic [33–40]. This

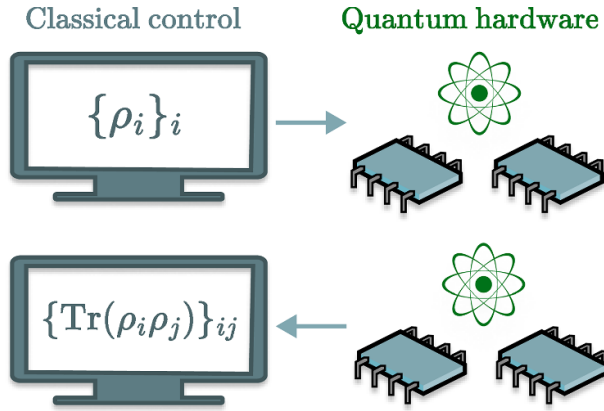


Figure 1. Pictorial description of our protocol. An experimentalist uses a quantum processing unit (QPU) to evaluate two-state overlaps $r_{i,j} = \text{Tr}(\rho_i \rho_j)$ for a given set of states either generated by that same QPU or by a state-preparation device of a third party. With this information, and using the scheme we propose, they can benchmark nonclassical resources: nonstabilizerness, coherence, and Hilbert space dimension. This certification is agnostic to the procedure used by the QPU to compute the overlaps.

novel foundational understanding is at the core of the application we envision, allowing us to distribute a quantum certification protocol among various parties in a network of QPUs.

The structure of this paper is as follows. Section 2 contains all the background needed for the understanding of our work; section 2.1 introduces important aspects of the stabilizer formalism while section 2.2 reviews the overlap paradigm recently introduced in references [31, 32] and the notion of set coherence [33]. In section 3, we define our basis-independent formulation of magic which, as mentioned above, we dub *set magic* and provide some intuition for it. Afterward, in section 4, we show that set magic can be witnessed using certain two-state overlap inequalities. Section 5 pushes our results even further. There, we introduce the notion of *full set magic* and leverage its witnessing by certain inequalities to certify that, in a given set of states, all states but one are magic; moreover, all the magic states must differ from one another. Since nonstabilizerness is a well-studied topic, in section 6 we comment on different experimental implementations of our method, as well as on its robustness and scalability, and compare it with the existing literature on the subject. In section 7, we make some final remarks and discuss promising open research lines stemming from this work.

2. Background

2.1. Stabilizer subtheory

In this work, we will focus on the stabilizer subtheory of n -qubit systems. We say that a pure quantum state $|\psi\rangle$ is a stabilizer state when it is the eigenvector with eigenvalue +1 for all elements of a maximal abelian subgroup of the Pauli group \mathcal{P}_n . The Pauli group is formed by all possible n -qubit Pauli operators, multiplied by phases ± 1 and $\pm i$. The dynamics of this subtheory is described in terms of Clifford operations, defined to be those that preserve the Pauli group under conjugation, i.e. $C\mathcal{P}_nC^\dagger = \mathcal{P}_n$.

For many different architectures, it is relatively easy to perform Clifford operations and prepare stabilizer states. This subtheory is crucial to applications in fault-tolerant magic-state

injection schemes and quantum error correction, and much work has been done to understand its geometrical properties. García *et al* [41] showed that stabilizer states have a fixed overlap structure. Recall that any two pure states $|\psi\rangle, |\phi\rangle \in \mathcal{H}$ can be orthogonal ($|\langle\psi|\phi\rangle| = 0$), parallel ($|\langle\psi|\phi\rangle| = 1$), or oblique ($0 < |\langle\psi|\phi\rangle| < 1$). When two *pure* stabilizer states are oblique, their two-state overlap obeys the following:

Theorem 1 (Adapted from [41]). *Given two oblique n -qubit pure stabilizer states $|\psi\rangle$ and $|\phi\rangle$ their overlap is given by $|\langle\phi|\psi\rangle|^2 = 2^{-k}$ for some $k \in \{1, 2, \dots, n\}$.*

The convex hull of all n -qubit pure stabilizer states, for each fixed value of $n \geq 1$, forms a polytope that we will refer to as STAB. Any state outside of STAB is termed in the literature *magic* or *nonstabilizer* state¹¹. Theorem 1 presents a simple method for witnessing nonstabilizer states in *pure* states using overlaps: Any deviation from the values $1/2^k$ witnesses the presence of such a resource. Beyond that, purity allows efficient schemes to quantify nonstabilizer states. References [21, 23] provide *quantifying* protocols that are close to being optimally efficient. However, without the assumption of purity (which is never perfectly attained experimentally), any overlap is possible by states inside of STAB and the task of witnessing magic becomes non-trivial. The test we propose, although based on two-state overlaps, does not require purity of states.

2.2. Coherence based on two-state overlaps

Initially motivated by benchmarking various resources in linear optical devices—Hilbert space dimension [42], quantum coherence [42], indistinguishability [43, 44]—references [31, 32] proposed an inequality formalism based solely on linear functionals of two-state overlaps. These overlaps are defined by $r_{i,j} = \text{Tr}(\rho_i \rho_j)$ for any two states ρ_i and ρ_j over the same Hilbert space.

Consider edge-weighted graphs (\mathcal{G}, r) where $\mathcal{G} = (V(\mathcal{G}), E(\mathcal{G}))$ is a graph¹², and $r : E(\mathcal{G}) \rightarrow [0, 1]$ is a function. We refer to fully connected finite simple graphs \mathcal{G} as *event graphs*¹³, as introduced in [32]. Any $(r_e)_{e \in E(\mathcal{G})}$ is merely a tuple of numbers. We will be interested in the problem of deciding when the numbers $r_{i,j}$ in these tuples are realizable by quantum states, thus equating to $\text{Tr}(\rho_i \rho_j)$; this is an instance of a *quantum realization problem* [45]. More formally, let $\mathcal{D}(\mathcal{H})$ represent the set of all quantum states with respect to a system \mathcal{H} and consider a finite set of states $\underline{\rho} \equiv \{\rho_i\}_i \subset \mathcal{D}(\mathcal{H})$ where $\{\rho_i\}_{i=1}^m \equiv \{\rho_1, \dots, \rho_m\}$. Denote $r(\underline{\rho}) \equiv r(\{\rho_i\}_i) := (\text{Tr}(\rho_i \rho_j))_{\{i,j\} \in E(\mathcal{G})}$; we will refer to $r(\underline{\rho})$ as a *quantum realization* for a given edge-weight r . Tuples $r \in [0, 1]^{|E(\mathcal{G})|}$ can have any number of quantum realizations, including none at all [32].

We proceed to discuss the notion of coherence for a set of states [31, 33] that differs from the commonly described basis-dependent view on coherence [2, 3] and its witnesses [46–48]. It also differs from the basis-independent coherence discussed in [49–51] defined with respect to a single state ρ instead of sets $\underline{\rho}$.

¹¹ Some authors prefer to term ‘magic states’ only those nonstabilizer states that can be distilled using stabilizer operations [30]. Instead, we prefer to adhere to the terminology that *any* nonstabilizer state is a magic state.

¹² A graph is an ordered pair $(V(\mathcal{G}), E(\mathcal{G}))$ where $V(\mathcal{G}), E(\mathcal{G})$ are sets. The first set $V(\mathcal{G})$ is interpreted as a set of nodes (or vertices) for the graph, hence a simple set of labels. The second set $E(\mathcal{G})$ corresponds to elements of the form $e = \{i, j\}$ such that $i, j \in V(\mathcal{G})$, i.e. the edges of \mathcal{G} .

¹³ A finite graph is one in which $|V(\mathcal{G})| < \infty$. A simple graph is undirected, no pair of nodes can have more than one edge, and there exist no edges of the form $\{v, v\}$ for $v \in V(\mathcal{G})$. Finally, a fully connected graph is one in which for any two vertices v, w there exists a family of edges connecting the two.

Definition 1 (Set coherence [33]). Let $\underline{\rho} \subseteq \mathcal{D}(\mathcal{H})$ be a finite set of states and $d = \dim(\mathcal{H}) < \infty$. When there exists some unitary U such that $\underline{\rho}$ satisfies $U\underline{\rho}U^\dagger = \underline{\sigma}$ where $\underline{\sigma}$ is a set of diagonal density matrices, we say that the set of states $\underline{\rho}$ is *set-incoherent*¹⁴. Otherwise, we say that it is *set-coherent*.

Set coherence is a basis-independent property of a set of states. Importantly, for any event graph \mathcal{G} , it is possible to bound two-state overlaps r realized by incoherent set of states : in such cases, incoherent states in the set satisfy $\underline{\sigma} \ni \sigma = \sum_{\lambda \in \Lambda} \sigma_{\lambda\lambda} |\lambda\rangle\langle\lambda|$, for some \mathcal{H} with $d = \dim(\mathcal{H})$ and some basis $\Lambda = \{|\lambda\rangle\}_{\lambda=1}^d$.

For any fixed event graph \mathcal{G} , the set of all possible edge-weights r realizable by some set-incoherent $\underline{\sigma}$ forms a full-dimensional convex polytope, denoted by $\mathcal{C}(\mathcal{G})$ [32]. Some convex polytopes $\mathcal{C}(\mathcal{G})$ have been completely characterized for certain event graphs \mathcal{G} .

The facet-defining inequalities for $\mathcal{C}(\mathcal{C}_m)$, with \mathcal{C}_m the cycle graph of m -nodes, were presented in [31] and are the so-called m -cycle inequalities

$$c_m(r) := -r_e + \sum_{e' \neq e} r_{e'} \leq m-2, \quad \text{for each } e \in E(\mathcal{C}_m). \quad (1)$$

For any convex-linear functional $h(r)$, we denote $h(r(\underline{\rho}))$ its value attained by some quantum realization $r(\underline{\rho})$. Violations $c_m(r(\underline{\rho})) > m-2$ witness the impossibility of the overlaps to be realized by incoherent sets of states, i.e. they witness set coherence of any such $\underline{\rho}$.

Another relevant family of inequalities, defined recursively, is the following:

$$h_m(r) = h_{m-1}(r) + r_{1m} - \sum_{i=2}^{m-1} r_{im} \leq 1. \quad (2)$$

The sequence above starts with $h_3(r) = r_{12} + r_{13} - r_{23} \equiv c_3(r)$ and defines novel inequalities for any integer $m > 3$. Each h_m inequality was shown in [32] to be facet-defining for the polytope $\mathcal{C}(\mathcal{K}_m)$, where \mathcal{K}_m is the complete graph with m nodes. It has been shown for up to 12-qubit systems that $h_m(r) \leq 1$ cannot be violated by sets $\underline{\rho} \subseteq \mathcal{D}(\mathbb{C}^d)$ where $d \leq m-2$ [52]. Numerically, we can see maximal quantum violations for m states $\underline{\rho}$ with dimension $d \geq m-1$.

3. Generalizing nonstabilizerness to set of states

We start the presentation of our main results by introducing the notion of *set magic* or *set nonstabilizerness*.

Definition 2 (Set magic). Let $\underline{\rho} \subseteq \mathcal{D}(\mathcal{H})$ be a finite set of states and $d = \dim(\mathcal{H}) < \infty$. We say $\underline{\rho}$ is *set-magic* or *set-nonstabilizer* when there exists no unitary $U : \mathcal{H} \rightarrow \mathcal{H}$ such that $U\underline{\rho}U^\dagger = \underline{\rho}'$ is a set of states within the stabilizer polytope.

Set magic implies the nonstabilizerness of *some* element in the set. Notably, the converse is *not* true, as we will see in an example below. Definition 2 above is a straightforward translation of set coherence [33] to the context of nonstabilizerness as a quantum resource. In section 5, we will show that, under certain conditions, it is possible to bound the number of states $\rho \in \underline{\rho}$ that are outside of STAB, instead of merely witnessing that some are.

Set magic and set coherence behave differently. Given any basis-dependent coherent pure state $|\psi\rangle$, with respect to some basis of reference $\{|i\rangle\}_i$, we have that $\{|\psi\rangle, |i\rangle\}$ must be

¹⁴ Equivalently, a set of states is incoherent iff all its elements pairwise commute.

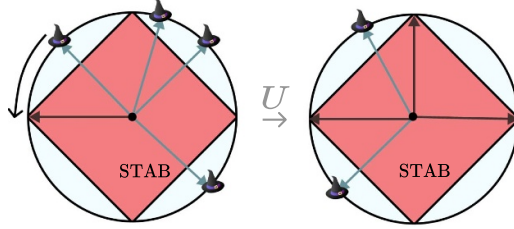


Figure 2. Geometrical interpretation of set magic. Consider we have a set of pure, single-qubit states that lie in a great circle of the Bloch sphere so that their projection in this great circle is depicted in the figure. If there is some unitary U that, when applied to the set of states, rotates them so they all lie inside the stabilizer polytope, then the set is said to be set-stabilizer (in this precise, basis-independent way). If this is impossible, the set is set-magic. This geometric picture allows some additional observations. Notably, by changing how the states are represented, one can often transform set with many magic states into one with fewer such states while preserving all relational properties (in this case, their arrangement in the Bloch sphere). As an example, on the left of the figure, we have a set with four magic states, but a suitable unitary operation can substitute this for a set with only two magic states. Importantly, our method is not restricted to pure states but applies also to mixed states. We will see later (section 5) that our techniques can be fine-grained to allow the identification of sets such that only *one* state can ever be mapped inside of STAB.

set-coherent. In contrast, given a magic state $|\phi\rangle$ and a stabilizer state $|s\rangle \in \text{STAB}$, the set $\{|\phi\rangle, |s\rangle\}$ need *not* necessarily be set-magic. For example, the set $\{|0\rangle, |T\rangle\}$, with $|T\rangle := (|0\rangle + e^{i\pi/4}|1\rangle)/\sqrt{2}$, is *not* set-magic since

$$\{|0\rangle\langle 0|, |T\rangle\langle T|\} \xrightarrow{T} \{|0\rangle\langle 0|, |+\rangle\langle +|\} \subset \text{STAB},$$

where $T := \text{diag}(1, e^{i\pi/4})$. However, the same set clearly has nonstabilizerness in the usual sense, something that can be seen if we restrict global unitaries to be Clifford unitaries, i.e. $\forall C$ belonging to the Clifford group:

$$\{|0\rangle\langle 0|, |T\rangle\langle T|\} \xrightarrow{C} \{|\psi_1\rangle\langle\psi_1|, |\psi_2\rangle\langle\psi_2|\} \not\subset \text{STAB}.$$

Set magic is therefore a more restricted notion than magic itself, being a property of the whole set of states. Figure 2 provides a geometrical interpretation of set magic and set stabilizerness: Given a set of states, if it is *impossible* to rotate it so that all states ‘fit’ inside the stabilizer polytope, we have set magic.

4. Certifying nonstabilizerness

In any certification protocol, the assumptions behind the test play a central role. In our case, we assume (a) multi-qubit or multi-qudit systems and (b) the ability to estimate two-state overlaps. Our test can be understood within the framework of prepare-and-measure scenarios as a semi-device-independent technique [53, 54]. This kind of statistics can also be self-tested [55]. The exact way in which this estimation is obtained may be unknown. Common techniques involve performing SWAP tests, Bell measurements, or generating specific prepare-and-measure statistics (more comments on this are deferred to section 6.1). Minimizing sample and measurement complexity is desired for scalability, although not essential for the certification *per se*. Commonly, a minimal requirement is using a number of samples and measurements smaller than the one needed to make (ideal) quantum state tomography [56–60], which

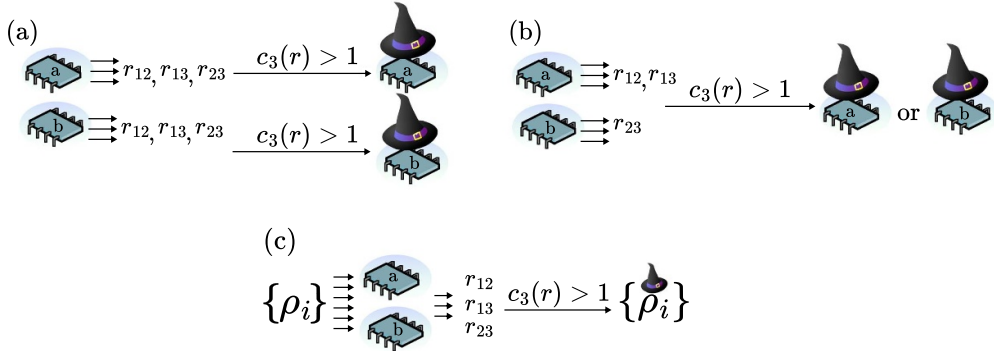


Figure 3. Certifying nonstabilizerness using two-state overlaps. (a) One can use our inequality witnesses for each device individually. (b) In case it is not necessary to certify that all devices have nonstabilizerness, but that *some do*, it is possible to reduce the time usage by distributing the overlap computation. (c) A third party sends states to be certified by the QPU network, that now serves as a tool for generating overlap statistics. With this information, one can witness nonstabilizerness in the provided set. We use $c_3(r)$ as an example, but the same remains valid for $c_m(r)$ violations.

is of order $O(d_T^2/\varepsilon^2)$, where ε is a fixed precision with respect to distance functions and d_T is the dimension of the whole Hilbert space considered. For QPUs with n qubits and associated Hilbert space $\mathcal{H} = (\mathbb{C}^2)^{\otimes n}$, a network of $s \in \mathbb{N}$ such units has space $\mathcal{H}^{\otimes s}$, implying $d_T = \dim(\mathcal{H}^{\otimes s}) = 2^{sn}$.

As shown in appendix A, event-graph inequalities cannot witness nonstabilizerness in general. This is somewhat unsurprising, as they were not proposed for such a task. However, we show that *some* event-graph inequalities *are* witnesses of both nonstabilizerness and coherence, starting with the cycle inequalities.

Theorem 2. *Every cycle inequality violation $c_m(r) > m - 2$ is a robust witness of nonstabilizerness for any set $\underline{\rho}$ of multi-qubit states such that $r = r(\underline{\rho})$.*

Importantly, theorem 2 holds for any set of multi-qubit states and not only for pure states. In appendix B, we use semidefinite programming (SDP) techniques [54] to find the maximal quantum violations of the cycle inequalities for $m = 3, 4, 5, \dots, 20$ and show that these are attained by single-qubit systems. It has been conjectured in [31] that all such inequalities are maximally violated by sets of single-qubit pure states and our numerical investigations suggest that this is indeed the case. In appendix C, we show that all facet-defining overlap inequalities for $\mathcal{C}(\mathcal{G})$, for any event graph \mathcal{G} , are maximally violated by sets of pure states and use this to prove theorem 2.

Theorem 2 leads to three different certification procedures. Suppose we have a network with s distinct units. The first method is illustrated in figure 3(a). Each individual QPU is used to prepare certain states and output all the corresponding two-state overlaps. Violation of the chosen inequality witnesses that each individual QPU resorted to magic resources in the preparation of the states.

The second method is illustrated in figure 3(b). We can distribute the state preparation and overlap estimation across different units, reducing the number of overlaps that need to be evaluated in each QPU. This certifies that the network as a whole can generate nonstabilizerness

somewhere across its parties. Compared to other protocols [24, 25] ours has the advantage that it foregoes the need to entangle the different QPUs in the network to carry out this certification.

Comparing these two schemes, suppose that the certification of each unit—as seen in figure 3(a)—requires the evaluation of m overlaps. The first method requires a total of $s \times m$ overlaps to be estimated, while for the second method, the evaluation of m overlaps suffices to certify the entire network for the presence of nonstabilizerness.

The second method is more useful than the first in the following scenario. Suppose that, in a network having a total of s QPUs, only a single (unknown) QPU is capable of generating nonstabilizer resources. Running method (a) on a single (randomly chosen) QPU has a probability of success of $1/s$ of detecting the presence of magic, whilst the distributed certification always succeeds. In section 5, we will show that, in some cases, this same procedure can enable an even stronger certification, allowing us to guarantee that *all but one* QPU have produced nonstabilizer resources.

The third method is depicted in figure 3(c). Suppose we are supplied with a set of m unknown states provided by third parties and are asked the question: Is the set magic? In this case, the network is not the object being investigated, but a useful tool for certifying the states provided by the third parties. We can use our network to answer this question by distributing the estimation of the overlaps among any number of the available QPUs.

In section 6.3, we provide a comprehensive comparison between our approach and other protocols in the literature.

Cycle inequalities certify the presence of nonstabilizerness but, as stated above, they are always maximally violated by sets $\underline{\rho} \subseteq \mathcal{D}(\mathbb{C}^2)$ of single-qubit states. This feature implies that such a certification scheme is not capable of capturing genuine properties of multi-qubit nonstabilizer resources, i.e. magic states in $\mathcal{D}(\mathbb{C}^{2^n})$.

To address the possibility of witnessing nonstabilizerness that necessitates having access to higher Hilbert space dimensions, we study inequalities that witness *both* of these properties. The simplest example of such inequalities is $h_4(r) \leq 1$ which, as shown in [52], requires two-qubit systems (or single qutrits) to have a violation. We complement this result by showing that violations of $h_4(r) \leq 1$ also witness nonstabilizerness.

Theorem 3. *The inequality $h_4(r) \leq 1$ cannot be violated by quantum realizations $r = r(\underline{\rho}_{\text{STAB}})$ of sets of stabilizer states $\underline{\rho}_{\text{STAB}}$.*

We defer the proof of this result to appendix D.

5. Full set magic

We have seen that our inequality witnesses can be used to signal the set magic of an arbitrary set of states $\underline{\rho}$. This indicates that *some* state(s) in $\underline{\rho}$ must be nonstabilizer. It is therefore natural to ask whether it is possible to certify a lower bound on the number of states that must always lie outside of STAB. Clearly, for any set $\underline{\rho}$, at least one state ρ_{ref} can always be unitarily mapped inside STAB. With this in mind, we introduce the following notion.

Definition 3 (Full set magic). Let $\underline{\rho} \subseteq \mathcal{D}(\mathcal{H})$ be a finite set of states, $d = \dim(\mathcal{H}) < \infty$. We say that the set $\underline{\rho}$ is *fully set magic* or *fully set nonstabilizer* if, for every unitary $U : \mathcal{H} \rightarrow \mathcal{H}$, all states (but one) lie outside of the stabilizer polytope.

There exist sets of states with full set magic. Let $\mathcal{H} = \mathbb{C}^2$ and consider any triplet of states $\{\rho_1, \rho_2, \rho_3\}$. It can be shown numerically that $c_3(r(\underline{\rho})) \leq 1.21$ if at most one state in $\underline{\rho}$ is outside of STAB. Recall that the maximal value of c_3 achieved with generic quantum states is 1.25.

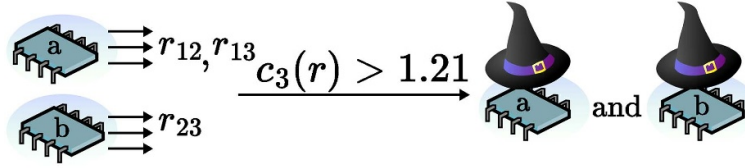


Figure 4. Certifying magic in many QPUs with a single witness. Fixing a certain target dimensionality (in this case single-qubit systems), one can certify all elements in a network from the same inequality values. Equivalently, one can certify various qubits in the same quantum computer running a parallel computation of the inequality values.

Table 1. Full set magic bounds. The first column shows the cycle inequality considered and the second column shows the corresponding optimal value considering quantum realizations of sets of states $\underline{\rho} \subseteq \mathcal{D}(\mathbb{C}^2)$ where at least two states $\rho_i, \rho_j \in \text{STAB}$. The last column presents the optimal tight values found in appendix B. Interestingly, even cycles cannot witness full set magic, but odd cycles can.

m	3	4	5	6	7	8	9
c_m	1.2071	2.4142	3.5061	4.5981	5.6468	6.6955	7.7254
c_m^{\max}	1.2500	2.4142	3.5225	4.5981	5.6534	6.6955	7.7286

Note that, for analyzing full set magic, we fix the dimension. Therefore, there may be multi-qubit systems realizing values larger than $c_3(r) = 1.21$ while having only one nonstabilizer state. Figure 4 depicts how this result can be explored to implement a protocol that certifies a set of states for the presence of full set magic.

Although above we focus on the simplest example of the c_3 inequality, we present numerical evidence that other odd cycle inequalities can be also used to witness full set magic. As can be seen from table 1, depending on how large the violation of $c_m(r(\underline{\rho})) \leq m - 2$ is, we have that, other than one reference state that can always be unitarily sent inside STAB, all the other $m - 1$ states must be magic states. Moreover, all of these states must be different, otherwise it would be possible to map two states inside of STAB. The second column from table 1 is obtained as follows. We assume that there are at least two states in a set $\{|\psi_i\rangle\}_{i=1}^m$ that are single-qubit stabilizer states. Without loss of generality, we can consider only the pairs $\{|0\rangle, |+\rangle\}$ or $\{|0\rangle, |1\rangle\}$. All the remaining $m - 2$ states are generic single-qubit states of the form $|\psi_i\rangle = \cos(\theta_i)|0\rangle + e^{i\phi_i} \sin(\theta_i)|1\rangle$. For all possible combinations of $m - 2$ generic states with the two chosen stabilizer states (or, equivalently, all possible edge $\underline{\psi}$ -labelings of the graph \mathcal{C}_m permuting the two stabilizer states), we maximize c_m with respect to the variables $\underline{\theta} = \{\theta_i\}_i$ and $\underline{\phi} = \{\phi_i\}_i$.

The tool used for the maximization was **NMaximize** of Wolfram Mathematica and all available solvers were tested; the final results correspond to the one that found the largest value. Note that, as before, even though we are maximizing for pure states, the results presented in table 1 hold for generic mixed states.

The last column of table 1 corresponds to the situation wherein the set is allowed to be full set magic, i.e. all states but one are nonstabilizer states. We can see that the gap between set magic and full set magic decreases as m increases. Interestingly, we cannot witness full set magic for even cycle inequalities since $m - 2$ magic states are sufficient to maximally violate the inequality.

6. Experimental schemes

6.1. Different strategies for implementing our test

We take this opportunity to discuss different strategies for evaluating two-state overlaps. One option is to consider prepare-and-measure estimation. In this case, a preparation stage prepares states $|\psi_i\rangle = U_i|0\rangle$, while a measurement stage acts as a projection onto $\langle\psi_j| = \langle 0|U_j^\dagger$. Assuming we are in the regime of full set magic, each overlap inequality will certify the non-stabilizerness of all the preparations U_i and all measurements U_j except one.

Another possibility is to use the SWAP-test [61] which, despite using a magic gate (the Fredkin gate), can unambiguously witness nonstabilizerness of the quantum states that are sent by a third party (sender). If we want to avoid the use of auxiliary qubits and magic operations to estimate the overlaps, we can instead use Bell measurements [21].

Finally, in the context of linear-optical implementations, we can use the Hong-Ou-Mandel effect [62]. Any linear-optical interferometer that is insensitive to internal degrees of freedom of the photons (e.g. polarization, frequency, time of arrival) has outcomes determined only by unitary-invariant properties of the spectral functions describing them [42, 63]. This means the Hong-Ou-Mandel effect, or interferometry in more complex multimode interferometers, can be used to directly estimate those invariant properties. Such a test could be used to certify the nonstabilizerness of these states.

6.2. Robustness and scalability

The inequalities $c_m(r) \leq m - 2$ and $h_4(r) \leq 1$ are our main magic witnesses. By default, they are both *robust to incoherent noise* and *scalable*. Robustness follows from the fact that they remain valid witnesses if, rather than pure states, we consider any set of states. Specifically, any state inside STAB cannot violate these inequalities. On the other hand, scalability stems from the fact that (i) two-state overlaps are well-defined independently of any Hilbert space dimension and (ii) quantum computers can efficiently estimate overlaps [64]. We refer to a protocol as scalable, or efficient, if one does not require exponentially increasing computational time, number of measurements, or samples. Additionally, in our case, it is clear that scalability will also depend on the trade-off between dimension and number of overlaps estimated in a given inequality, for instance estimating $h_{2^n}(r)$ is certainly *not* efficient.

6.3. Comparison with other schemes

In this section, we make a comprehensive review of existing methods for witnessing the non-stabilizerness of quantum states and compare them with our approach. Clearly, any *quantification* scheme also constitutes a witness, thus, for a broader comparison, we were careful to include such methods as well.

6.3.1. Methods that require additional entanglement generation. We start by presenting two witnessing schemes that require additional entanglement; they use multifractal flatness [25] and entanglement spectrum flatness [24]. First, define the inverse participation ratio,

$$I_q(|\psi\rangle) := \sum_{b \in \mathbb{F}_2^n} |\langle b|\psi\rangle|^{2q} = \sum_{b \in \mathbb{F}_2^n} r_{b,\psi}^q,$$

where \mathbb{F}_2^n denotes the n -dimensional vector space over the finite field \mathbb{F}_2 with two elements: 0 and 1. That is: $\mathbb{F}_2^n = \{(b_1, \dots, b_n) \mid b_i \in \{0, 1\} \text{ for all } i = 1, \dots, n\}$. We note that, to calculate

$I_q(|\psi\rangle)$ for any fixed q , one needs to evaluate $d = 2^n$ overlaps. The *multifractal flatness* is defined as

$$\mathcal{F}_{\text{multi}}(|\psi\rangle) := I_3(|\psi\rangle) - (I_2(|\psi\rangle))^2.$$

This quantity witnesses nonstabilizerness whenever we obtain $\mathcal{F}_{\text{multi}}(C|\psi\rangle) > 0$, where C is an n -qubit Clifford operation. Since both calculating and measuring this quantity require $O(d)$ overlaps, this witnessing process is inefficient. We remark that, when averaged over the Clifford orbit of the state $|\psi\rangle$, this witness provides information about the stabilizer Rényi entropy M_2 which we will discuss in more detail below.

Three key aspects of this witness stand in stark contrast to our scheme. First, it is device-dependent. Secondly, it is only applicable to pure states. Finally, to properly witness nonstabilizerness of $|\psi\rangle$, it requires additional entangling gates to be applied over the state $|\psi\rangle$, stemming from the Clifford unitary, C , needed for $\mathcal{F}_{\text{multi}}(C|\psi\rangle) > 0$.

Another function that can be used to witness nonstabilizerness is the *entanglement spectrum flatness* $\mathcal{F}_A(|\psi\rangle)$. We consider a pure state $|\psi\rangle$ ¹⁵ and some n -qubit Clifford operation C such that $C|\psi\rangle$ is sufficiently entangled. In some cases, shallow Clifford evolutions are enough. We then choose an arbitrary bipartition $\mathcal{H}_A \otimes \mathcal{H}_B \simeq \mathbb{C}^{\otimes n}$ of the n -qubit system and calculate $\rho_A := \text{Tr}_B(C|\psi\rangle\langle\psi|C^\dagger)$. The entanglement spectrum flatness of this bipartition is given by

$$\mathcal{F}_A(C|\psi\rangle) := \text{Tr}(\rho_A^3) - [\text{Tr}(\rho_A^2)]^2.$$

If we obtain that $\mathcal{F}_A(C|\psi\rangle) > 0$, $|\psi\rangle$ must be a magic state, and therefore $\mathcal{F}_A(C|\psi\rangle) > 0$ acts as a witness of nonstabilizerness. This witness can be efficiently measured (in terms of the number of measurements and samples of ρ_A required) using simple quantum circuits [39, 65, 66].

Let us discuss more explicitly the advantages and drawbacks of these techniques when compared to the scheme we propose. Entanglement spectrum flatness has the advantage that it can witness almost any magic state (in the sense of Haar random states). In contrast, in our inequality-based witness, certifications should target certain overlap values that become increasingly rare for large systems to access randomly. This happens since the two-state overlap between Haar random n -qubit states behaves as $r_{i,j} \sim 1/2^n$. Moreover, both flatness results from above can approximate values of nonstabilizer monotones; thus, they can ultimately be used for quantification (a task strictly more powerful than witnessing). At the moment, our protocol has no known link with quantification tools, although we believe this to be an interesting direction for future research.

On the other hand, unlike our scheme, both of these methods are device-dependent and applicable only to pure states. Additionally, let us assume that we would like to certify the generation of nonstabilizerness in *some* QPU of a network. Figure 3(b) illustrates our proposal to handle this task. Notably, as previously explained, the certification can be distributed requiring fewer resources than if we were to certify each QPU individually (figure 3(a)). Contrastingly, with either of the two witnesses presented here, distributing the certification requires us to entangle the degrees of freedom of the multiple QPUs in the network we are interested in certifying, due to the Clifford operations that must be applied.

6.3.2. Methods that require full information about the STAB polytope or about the quantum state. The vast majority of quantification schemes require full information on the stabilizer

¹⁵ Tirrito *et al* [24] exemplifies the task using an n -qubit fully separable state, but, to the best of our understanding, their protocol works for any state.

polytope. Beyond that, they often also require full (tomographic) information of the quantum state. The following monotones require complete knowledge of the underlying state *and* of the STAB polytope: stabilizer fidelity [27], stabilizer extent [27], stabilizer rank [27–29], stabilizer nullity [67]. Some that are also well-defined for generic mixed states, having the same drawbacks, are mana [30, 68], all variations of the robustness of magic [69], relative entropy [30], min- and max-relative entropies [26], and dyadic negativity [69].

It is interesting to remark that the stabilizer extent $\xi(|\Psi\rangle)$ has the extremely useful property of being multiplicative,

$$\xi(|\Psi\rangle) := \xi(|\psi_1\rangle \otimes \cdots \otimes |\psi_m\rangle) = \prod_{j=1}^m \xi(|\psi_j\rangle),$$

provided that all states $|\psi_j\rangle$ are 1-, 2- or 3-qubit states, i.e. that $\psi \subseteq \mathcal{D}(\mathbb{C}^{2^s})$ with $s \in \{1, 2, 3\}$ [27]. This implies that an alternative strategy to witnessing nonstabilizerness is to make 1-, 2-, or 3-qubit state tomography of all states $|\psi_j\rangle$, use that information to calculate their stabilizer extent, and then multiply the results. Compared to our scheme, beyond being significantly device-dependent and demanding great control of the system (since one must perform full tomography), our scheme requires a smaller number of measurements and samples (since overlap estimation is experimentally less demanding than performing full tomography, even for single-qubit systems). It has been shown that the stabilizer extent is *not* multiplicative in general [70]. It is also clear that, for larger systems, our witnessing technique will outperform any strategy that demands full-state tomography.

The stabilizer nullity can be extended to treat unitaries [71]. In this form, it gives a lower bound to the number of T gates required to apply a certain unitary. A similar property holds for other magic monotones. Bounding the number of T gates is not possible with our formalism, as this is a profoundly basis-dependent characterization.

It is noteworthy that several of the quantifiers mentioned above have been associated with the perspective of witnessing as can be seen in [69]. Therein some witnesses for single-qubit magic states were proposed. Additionally, the authors also show curious lower and upper bounds on the scaling of magic monotones as the number of qubits n grows.

Interestingly, Rall *et al* [72] introduces a quantity called the *stabilizer norm*, defined as

$$\mathcal{S}(\rho) = \frac{1}{2^n} \sum_{P \in \mathcal{P}_n} |\text{Tr}(\rho P)|,$$

and shows that it can be used to witness nonstabilizerness, even for generic mixed states of multi-qubit systems. The function \mathcal{S} is multiplicative under tensor products and is upper bounded by the robustness of magic. The authors use this construction to describe what they refer to as ‘hyperoctahedral states’—states satisfying $\mathcal{S}(\rho) \leq 1$ —which are particularly interesting because they are nonstabilizer mixed states that admit fast classical simulation.

6.3.3. Methods that are not valid for generic mixed states. To the best of our knowledge, various quantifiers have not been generalized beyond pure states; examples of these include stabilizer fidelity, stabilizer rank, and stabilizer nullity. On the other hand, the stabilizer extent has a mixed state version [69].

Recall that if one assumes purity of states and multi-qubit systems, a trivial witness is to measure a single overlap of the state with respect to the $|0^n\rangle$ state, in which case deviations from $1/2^n$ will witness nonstabilizerness. Because of that, it is only quantification that proves to be a non-trivial task in the case of multi-qubit pure states. Therefore, in this section, we focus on quantification methods that are, in some way, efficient to calculate or measure, at

the cost of being defined only for pure states (or specific classes of mixed states). The stabilizer entropies are the most relevant measures in this category. The first such entropy introduced was the stabilizer Rényi entropy [73]. Generally speaking, these are inefficient to *compute* (not necessarily to *experimentally measure*) with respect to the number of qubits n of the quantum system. Haug and Piroli [74] investigated when such functions can be considered monotones and provided an explicit case study where stabilizer entropies could be computed efficiently. Haug *et al* [23] introduced novel stabilizer entropies and algorithms for their efficient measurement provided the α -moment of the Pauli spectrum of the quantum state under consideration scales inversely polynomially with n .

It is simple to see for the case of stabilizer Rényi entropies why the quantifiers do not hold for generic mixed states. Let us consider, for instance, the stabilizer 2-Rényi entropy defined for mixed states $\rho \in \mathcal{D}(\mathbb{C}^2)$ as

$$\tilde{M}_2(\rho) := -\log_2 \left(\frac{\sum_P [\text{Tr}(P\rho)]^4}{2\text{Tr}(\rho^2)} \right)$$

where the sum is taken over the +1 elements of the single-qubit Pauli group $\{\mathbb{1}, X, Y, Z\}$. Crucially, \tilde{M} is *not* a monotone for any mixed state ρ , but only for those with a specific form, given by $\rho = \frac{1}{2} + \frac{1}{2} \sum_{P \in G} \phi_P P$ where G is a subset of the single-qubit Pauli group, and $\phi_P \in \{-1, 1\}$ [73]. For instance, considering the magic state

$$|F\rangle\langle F| = \frac{1}{2} \left(\mathbb{1} + \frac{1}{\sqrt{3}} (X + Y + Z) \right)$$

and mixed states $\rho_\nu = \mathcal{E}_\nu(|F\rangle\langle F|) = (1 - \nu)|F\rangle\langle F| + \nu \frac{1}{2}$, the monotone as a function of ν becomes

$$\tilde{M}_2(\rho_\nu) = -\log_2 \left\{ \frac{1 + 3 \left[(1 - \nu) / \sqrt{3} \right]^4}{1 + 3 \left[(1 - \nu) / \sqrt{3} \right]^2} \right\}.$$

Since $\tilde{M}_2(\rho_\nu) > 0$ for any $\nu > 0$, it is not a faithful monotone (or witness), since it would signal the presence of nonstabilizerness for states arbitrarily close to the maximally mixed state.

Despite not being defined for mixed states, these monotones are extremely promising ways of efficiently estimating nonstabilizerness. For instance, [21, 75] estimated nonstabilizerness in a cloud-available quantum computer. Haug *et al* [23] showed that there are stabilizer entropies that can be *efficiently measured*, with the required number of measurements (or post-processing) being independent of system size. Finally, [21] introduced a novel monotone, which the authors termed ‘Bell magic’ that, besides being efficiently estimated on a quantum computer via Bell measurements, also generalizes to certain sets of mixed states. Bell magic was recently measured in [76].

6.3.4. Methods that are semi-device independent. Due to the connection between nonstabilizerness, the negativity of quasiprobability distributions, and noncontextuality (both Kochen–Specker and generalized), under certain considerations, any test of such notions of classicality will also be a test capable of witnessing nonstabilizerness. This is discussed in detail in appendix A; here, we comment on the device- or semi-device-independent nature of these tests.

Our witnesses are inequality-based and semi-device independent in the sense that (i) the test is made based only on statistics arising from two-state overlaps and (ii) we assume (in most cases) that the underlying system is a multi-qubit system. These restrictions are the ‘semi’ for

our approach. Inequalities that can be used to witness noncontextuality are significantly more device-independent, in the sense that they are not necessarily overlap-based (or correlation-based), while they will necessarily require some prior information about the Hilbert space considered: even, odd, odd-prime, or composite system dimensionality structures.

One subtle point needs to be made: Violations of noncontextuality inequalities *per se* do not suffice to experimentally witness the failure of noncontextual explanations of the data. One must also test that the experimental requirements relative to the notions of KS-noncontextuality or generalized noncontextuality are operationally met. Similarly to Bell inequality violations, merely violating them does not attest to the failure of a local explanation of the data; some minimal requirements need to be met (such as space-like separation between parties, no-signaling, etc). In our case, the requirement is that the data is described by two-state overlaps, while in noncontextuality inequalities other requirements are needed, and should be taken into consideration, even if one is only interested in witnessing nonstabilizerness due to contextuality.

7. Discussion and future directions

We have shown that some two-state overlap inequalities that have been recently introduced and successfully applied to investigate, theoretically and experimentally, a wide range of non-classical resources [31, 39, 42–44, 52, 77, 78] are also nonstabilizerness witnesses. Using this framework, we develop certification methods applicable to a single QPU, networks of QPUs, and a form of delegated certification of states shared by third parties. Our witnesses are robust in the sense of applying to both pure and mixed states of any kind. They are also scalable, meaning they are independent of the system’s dimension.

It is worth mentioning that, arguably, a major drawback of our protocol is that, for multi-qubit systems, violations of the inequality become increasingly *rare* in the following sense: Haar-random pure quantum states of many qubits have an exponentially decreasing probability of violating the witnesses we propose, simply because in such cases, quantum two-state overlaps scale as $\text{Tr}(\rho\sigma) \sim 1/2^n$. We expect this to remain true even if other inequalities from the event graph polytope are later shown to serve as nonstabilizerness witnesses. Future work could explore whether incorporating higher-order invariants might help to address this limitation.

Various of the tools put forward either have their own technical interest or present novel theoretical opportunities. For instance, set magic and full set magic can be further investigated within the resource-theory framework. In this paper, set magic arises naturally from using unitary invariants as our witnesses. There are several open questions on the possible operational importance of these results for quantum computation. Is it possible to connect set magic to the hardness of classically simulating a stabilizer circuit given a specific set of input states? Put differently, can set magic be a good signature of quantum computational advantage? Does a suitable *quantifier* for set magic exist? Framing simulation within a unitary-invariant framework could better pinpoint the resources responsible for the exponential overhead of classical simulation and even lead to a unified view of different simulation schemes [79].

In parallel, after the release of our paper, two other works [80, 81] have proved related results, highlighting the growing interest in connecting resource theories of magic with operational tests related to the violation of inequalities more commonly considered by the quantum foundations community. We believe our approach opens the door to a broader class of inequality-based tests—drawing on tools from quantum foundations, such as Bell and Kochen–Specker inequalities—that may also serve as witnesses of nonstabilizerness even for the case of multi-qubit systems. This perspective suggests promising new directions for identifying

and characterizing magic using foundational principles, similar to what has been investigated previously by [82–84].

In another direction, exploring if a similar effect to full set magic exists when considering the notion of set coherence could be of interest [31, 33]. Moreover, for composite systems, large violations of the inequality $h_4(r) \leq 1$ may also require the presence of entanglement. We believe these are aspects that merit further investigation.

Data availability statement

All data that support the findings of this study are included within the article (and any supplementary files).

Acknowledgments

We would like to thank Raman Choudhary, Mark Howard, Constantino Budroni, Lorenzo Leone, Salvatore F.E. Oliviero, and Alioscia Hamma for useful discussions. FCRP and RW acknowledge support from FCT—Fundação para a Ciência e a Tecnologia (Portugal) through PhD Research Scholarship 2020.07245.BD and PhD Grant SFRH/BD/151199/2021, respectively. FCRP also acknowledges funding by Ayuda Consolidación CNS2023-145392 funded by MICIU/AEI/10.13039/501100011033 and European Union NextGenerationEU/PRT. RW acknowledges support from the European Research Council (ERC) under the European Union’s Horizon 2020 research and innovation programme (grant agreement No. 856432, HyperQ). EZC acknowledges funding by FCT/MCTES through national funds and, when applicable, co-funding by EU funds under the project UIDB/50008/2020. EZC also acknowledges funding by FCT through project 2021.03707.CECIND/CP1653/CT0002. EFG acknowledges support from FCT via project CEECINST/00062/2018. This work was supported by the ERC Advanced Grant QU-BOSS, GA No. 884676.

Appendix A. Two-state overlap inequalities cannot witness nonstabilizerness in general

In this appendix, we will prove the existence of an event-graph inequality that is both facet-defining and violated by sets of stabilizer states. To do so, we use some results within the field of Kochen-Specker noncontextuality [7]. We then extend these considerations to generalized noncontextuality [85]. We also discuss how our findings compare with existing connections between contextuality and nonstabilizerness.

To provide some context, recall that magic-state injection is the leading model for experimentally realizing fault-tolerant quantum computation. While it involves only stabilizer operations at every step of the computation, the injection of magic states elevates the model to quantum universality. Howard *et al* [82] showed that contextuality is a necessary resource for universal quantum computation via magic-state injection. The scope of this result depends on whether the model involves even-prime dimensional qudits (i.e. qubits) or odd-prime qudits. For the latter case, a state is non-contextual if and only if it belongs to the set of states unable to unlock any computational speed-up. This set forms a polytope, denoted as \mathcal{P}_{SIM} , meaning that the subtheory within this polytope is efficiently simulable with classical computation. This polytope strictly contains the set of stabilizer states but is not equivalent to it.

Therefore, for odd-prime dimensions, Kochen–Specker noncontextuality inequalities serve as witnesses of nonstabilizerness. However, for even-dimensional systems, the same does *not* hold, as we now show. We start by constructing the relevant event graph. First, we construct the so-called *exclusivity graph* \mathcal{G}_{exc} [86, 87]. We take this graph to be the complement graph¹⁶ of the Shrikhande graph [88]. See [89, figure 2, pg 10] for a representation of \mathcal{G}_{exc} . We follow closely the discussion of the proof of KS-contextuality discussed in [89]. Secondly, we take the suspension graph [87, Definition 2.23, pg 36] $\nabla \mathcal{G}_{\text{exc}}$ by a new node \star . This new graph will be our event graph $\mathcal{G} = \nabla \mathcal{G}_{\text{exc}}$. It was shown in [32] that any inequality from an exclusivity graph \mathcal{G}_{ext} is mapped to some facet defining inequality of the event graph $\mathcal{G} = \nabla \mathcal{G}_{\text{exc}}$. Therefore, the inequality

$$\sum_{v \in V(\mathcal{G}_{\text{exc}})} r_{\star, v} \leq 3$$

is both a noncontextuality inequality (within the Cabello–Severini–Winter framework [86]) and a facet-defining event-graph inequality, when a specific mapping takes place (see [32] for details). This inequality corresponds to Mermin’s Bell inequality [90] and can be violated by letting the vertices $v \in V(\mathcal{G}_{\text{exc}})$ be given by the stabilizer (separable) states

$$\begin{aligned} & |0, +, +\rangle, |1, -, +\rangle, |1, +, -\rangle, |0, -, -\rangle \\ & |+, 0, +\rangle, |-, 1, +\rangle, |-, 0, -\rangle, |+, 1, -\rangle \\ & |+, +, 0\rangle, |-, -, 0\rangle, |-, +, 1\rangle, |+, -, 1\rangle \\ & |1, 1, 1\rangle, |0, 0, 1\rangle, |0, 1, 0\rangle, |1, 0, 0\rangle \end{aligned}$$

and \star by the Greenberger–Horne–Zeilinger (GHZ) state $|\text{GHZ}\rangle = \frac{1}{\sqrt{2}}(|0, 0, 0\rangle + |1, 1, 1\rangle)$. In this way,

$$\sum_{v \in V(\mathcal{G}_{\text{exc}})} r_{\star, v} = \sum_{v \in V(\mathcal{G}_{\text{exc}})} |\langle \text{GHZ}|v\rangle|^2 = 4 > 3.$$

The above shows that there are event-graph inequalities that can be violated by stabilizer states.

Let us now discuss the relationship between *generalized noncontextuality* [85] and nonstabilizerness. It was shown in [83, 84] that odd-dimensional stabilizer subtheory allows for a generalized noncontextual model. In this case, any violation of a noncontextuality inequality attesting to the failure of generalized contextuality will also be a witness of having states (transformations, measurement effects) outside the stabilizer subtheory. However, similarly to the case of KS-noncontextuality, for even-dimensional systems, no such noncontextual model for the stabilizer subtheory exists. Therefore, in general, even dimensional stabilizer subtheory *can* violate generalized noncontextuality inequalities. Finding which inequalities *are not* violated by such stabilizer subtheory becomes a case-by-case study.

In summary, the connection between event graph inequalities and noncontextuality inequalities does not imply that any event graph inequality will immediately be a nonstabilizerness witness and therefore does *not* render our results trivial. On the other hand, it also does not make our results immediately incorrect. The fact that our inequality witnesses (which can also be interpreted as noncontextuality inequalities) cannot be violated by stabilizer states does *not* imply that they do not violate *some* noncontextuality inequality. As it is in general, for

¹⁶ The complement of a graph \mathcal{G} is a new graph \mathcal{G}^c such that $V(\mathcal{G}) = V(\mathcal{G}^c)$ and, $e \in \mathcal{G}^c$ iff $e \notin \mathcal{G}$.

a given KS-measurement scenario (or equivalently, a generalized prepare-and-measure noncontextuality scenario), it is only if one satisfies *all* the noncontextuality inequalities that a noncontextual model exists.

Appendix B. Quantum bounds for magic witnesses

In this appendix, we investigate what are the optimal quantum violations of the inequality witnesses that we have proposed as nonstabilizerness witnesses. We start with a brief description of how SDP techniques can be used for such a task. We then use these tools to find the optimal quantum violations for the cyclic inequalities and the $h_4(r) \leq 1$ inequality.

B.1. Lower bounds

Let $f: \mathcal{D}(\mathcal{H})^{|V(\mathcal{G})|} \rightarrow \mathbb{R}$ be a convex-multilinear functional defined with respect to some facet-defining inequality of $\mathcal{C}(\mathcal{G})$, for some \mathcal{G} , i.e. $f(\cdot) \equiv h(r(\cdot))$. In its generic form, f is given by,

$$f(\rho) = \sum_{u,v \in V(\mathcal{G})} \alpha_{uv} \text{Tr}(\rho_u \rho_v),$$

where $\alpha_{uv} \in \mathbb{Z}$ for all u, v . We are interested in evaluating the quantum bound of this functional, i.e. $\max_{\{\rho_x\}_{x=1}^N} f$, over all possible quantum realizations, where $N = |V(\mathcal{G})|$.

To determine lower bounds for the quantum bound, we employ a seesaw of SDPs [91]. Indeed, by fixing all the states except one, the problem of maximizing the bound over the remaining state is an SDP task and can be performed efficiently.

B.2. Upper bounds

A way to evaluate upper bounds for this quantity is to adapt the Navascues-Vértesi (NV) hierarchy of SDP relaxations [92] to this particular problem. In a similar spirit, we make a list of operators $\mathcal{S} = \{\mathbb{1}, \{\rho_x\}\}$ and choose a degree of relaxation k . A relaxation of degree k consists of keeping all products of at most k operators from the list. The moment matrix is then constructed,

$$\Gamma_{ij} = \text{Tr}[S_i S_j],$$

where $S_i, S_j \in \mathcal{S}$. For a good introduction and review of SDP techniques in quantum information science see [91].

One samples a linearly independent basis of such moment matrices $\{\Gamma^{(1)}, \dots, \Gamma^{(m)}\}$. The relaxation then consists of finding an affine combination $\Gamma = \sum_{j=1}^m c_j \Gamma^{(j)} \in f$, with $\Gamma \geq 0$, as follows,

$$\max_{\vec{c} \in \mathbb{R}^m} f(\Gamma) \quad \text{s.t.} \quad \Gamma \geq 0, \quad \sum_{j=1}^m c_j = 1.$$

B.3. Maximal quantum violation of m -cycle inequalities

B.3.1. Qubit model. The optimal solution of the maximization problem for $c_m(r)$ is a set of states $\{|\psi_x\rangle\}_{x=1}^m$ of the form

$$|\psi_x\rangle = \cos(\theta_x^{(m)}) |0\rangle + \sin(\theta_x^{(m)}) |1\rangle. \quad (\text{B1})$$

where

$$\theta_x^{(m)} = \begin{cases} \frac{\pi}{2} - \frac{(x-1)\pi}{2m} & \text{if } m \text{ is odd,} \\ \frac{\pi}{2} + \frac{(x-1)\pi}{2m} & \text{if } m \text{ is even.} \end{cases}$$

This family of optimal states is found explicitly using the seesaw SDP technique. Using the hierarchy, we could prove that the quantum bound is tight (to 10^{-5} precision) for this family of states up to $m = 8$. For larger values of m , $m \leq 20$, we have checked the lower bounds match the analytical formula up to the same precision. For $m > 20$, we conjecture that this remains the optimal quantum solution.

B.3.2. Asymptotic behavior. Let us denote the set of optimal quantum states as $\underline{\psi}^{\max}$. The maximum quantum violation is then given by

$$c_m(r(\underline{\psi}^{\max})) = (m-1) \cos^2\left(\frac{\pi}{2m}\right) - \cos^2\left[\left(1 - \frac{1}{m}\right)\frac{\pi}{2}\right].$$

On the other hand, the optimal incoherent quantum realization is $c_m(r(\underline{\psi}^{\text{inc}})) = m-2$. The fraction between these two quantities goes to 1 as m grows.

Proposition 1. *The limit of the ratio $c_m(r(\underline{\psi}^{\text{inc}}))/c_m(r(\underline{\psi}^{\max}))$ when $m \rightarrow \infty$ is 1.*

Proof. To see this, write

$$\frac{c_m\left(r\left(\underline{\psi}^{\text{inc}}\right)\right)}{c_m\left(r\left(\underline{\psi}^{\max}\right)\right)} = \frac{m-2}{(m-1) \cos^2\left(\frac{\pi}{2m}\right) - \cos^2\left[\frac{1}{2}\left(1 - \frac{1}{m}\right)\pi\right]}.$$

The term $\cos^2\left(\frac{1}{2}\left(1 - \frac{1}{m}\right)\pi\right)$ is bounded, therefore the limit reduces to

$$\lim_{m \rightarrow \infty} \frac{c_m\left(r\left(\underline{\psi}^{\text{inc}}\right)\right)}{c_m\left(r\left(\underline{\psi}^{\max}\right)\right)} = \lim_{m \rightarrow \infty} \frac{m-2}{(m-1) \cos^2\left(\frac{\pi}{2m}\right)} = \lim_{m \rightarrow \infty} \frac{m-2}{m-1} = 1.$$

□

Figure 5 shows the ratio as a function of m , denoted, for simplicity, as C/Q . The numerics above suggest that pure single-qubit states always provide the optimal violation. We have numerically showed this to be true for m up to 20.

B.4. Maximum quantum violation of $h_4(r) \leq 1$

Again, using the methods described in this section, we can show tight bounds for the maximal quantum realizations violating $h_4(r) \leq 1$, for sets $\underline{\rho} \subseteq \mathcal{D}(\mathbb{C}^d)$ with $d = 3, 4$.

Note that h_4 (as any event-graph functional) satisfies $h_4(r(\rho)) = h_4(r(\underline{U}\rho\underline{U}^\dagger))$ for any unitary U and $\underline{U}\rho\underline{U}^\dagger \equiv \{U\rho_i U^\dagger\}_{i=1}^m$. This implies that any maximal quantum violation can be attained using Hilbert spaces of at most dimension $d = 4$. We find a tight bound of $1 + 1/3$, up to 10^{-5} precision, for both $d = 3, 4$, proving that qutrits are sufficient to achieve the maximum quantum violation of h_4 .

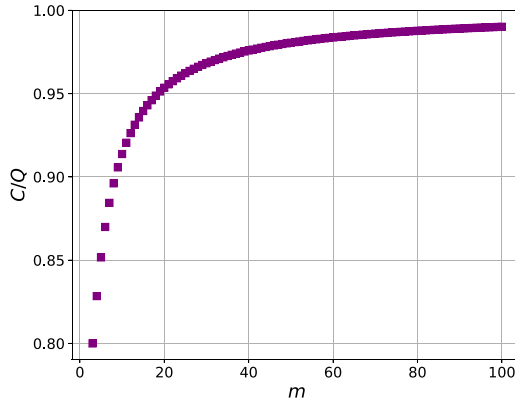


Figure 5. Asymptotic behavior of C/Q for the optimal solution of the cyclic inequalities. Here, $C \equiv m - 2$, which is the optimal value attainable by $c_m(r)$ with incoherent quantum realizations $r = r(\underline{\rho}^{\text{inc}})$. Q represents the optimal value obtainable using any quantum state, attained with $\underline{\rho} = \underline{\psi}^{\text{max}}$ given by equation (B1). We present their fraction as a (continuous) function of m .

Appendix C. Proof of theorem 2

Before proving theorem 2, we present some novel technical results that are of general interest to the event-graph formalism introduced in [32].

Following the same notation used, for any given event graph \mathcal{G} , with edges $E(\mathcal{G})$ and vertices $V(\mathcal{G})$, we denote the polytope of all edge-weights $r : E(\mathcal{G}) \rightarrow [0, 1]$ realizable by set-incoherent tuples as $\mathfrak{C}(\mathcal{G})$. The Hamming weight of a string (or, equivalently, a tuple) s of 0/1-assignments equals the number of 1 assignments in the string (or tuple) and is denoted $|s|_H$.

Lemma 4. *Let $\mathcal{G} = \mathcal{C}_m$ be the m -cycle graph. Fix $m \geq 3$ and some $\tilde{e} \in E(\mathcal{C}_m)$. If we denote*

$$\mathfrak{C}_{\tilde{e}} := \{r \in \mathfrak{C}(\mathcal{C}_m) : r_{\tilde{e}} = 1\},$$

we have that $\mathfrak{C}_{\tilde{e}} = \{1\} \times \mathfrak{C}(\mathcal{C}_{m-1})$.

This lemma shows that if we define the cross-section $\mathfrak{C}_{\tilde{e}}$ of the polytope $\mathfrak{C}(\mathcal{C}_m)$ along the direction $r_{\tilde{e}} = 1$, the resulting polytope is isomorphic to $\mathfrak{C}(\mathcal{C}_{m-1})$. This implies that given any facet-defining inequality of $\mathfrak{C}(\mathcal{C}_m)$, if we force an edge to be equal to one, the resulting inequality will be a facet-defining inequality of $\mathfrak{C}(\mathcal{C}_{m-1})$, or a trivial inequality.

Proof of lemma 4. Because $\mathfrak{C}(\mathcal{C}_m)$ is a convex polytope, the same is true for $\mathfrak{C}_{\tilde{e}}$. Let $\text{ext}(P)$ denote the set of extremal points of any convex polytope P , and hence $P = \text{CONVHULL}[\text{ext}(P)]$. Let us assume, wlog, an ordering $r = (r_e)_{e \in E(\mathcal{C}_m)} = (r_{\tilde{e}}, r_{e_1}, \dots, r_{e_{m-1}})$. We want to show that,

$$\text{ext}(\mathfrak{C}_{\tilde{e}}) = \{(1, s) \in \mathbb{R}^m : s \in \text{ext}(\mathfrak{C}(\mathcal{C}_{m-1}))\}.$$

(\subseteq) Let $\tilde{r} \in \text{ext}(\mathfrak{C}_{\tilde{e}})$. By construction, we must have that $\tilde{r} \equiv (1, \tilde{s}) \in \text{ext}(\mathfrak{C}(\mathcal{C}_m))$, with \tilde{s} a deterministic assignment for which $|\tilde{s}|_H \neq m - 2$. Therefore, $\tilde{s} \in \text{ext}(\mathfrak{C}(\mathcal{C}_{m-1}))$.

(\supseteq) This direction follows trivially.

Hence, we have that

$$\mathfrak{C}_{\tilde{e}} = \{1\} \times \mathfrak{C}(\mathcal{C}_{m-1}),$$

where $\{1\}$ is the singleton polytope, as we wanted. \square

This simple result will be instrumental for constructing the inductive step used in the proof of theorem 2.

We now make the notion of a quantum realization within the context of the event graph formalism precise. We can associate nodes of the graph to quantum states $V(\mathcal{G}) \ni v \xrightarrow{\ell} \rho_v \in \underline{\rho}$ via some vertex $\underline{\rho}$ -labeling $\ell : V(\mathcal{G}) \rightarrow \underline{\rho}$. Once such labeling ℓ is fixed, we associate edge-weights $r_e \equiv r_{u,v}$ to two-state overlaps $E(\mathcal{G}) \ni e = \{u, v\} \xrightarrow{\ell} \{\rho_u, \rho_v\} \xrightarrow{\langle \cdot, \cdot \rangle_{\text{HS}}} \text{Tr}(\rho_u \rho_v)$ ¹⁷, with $\langle X, Y \rangle_{\text{HS}} = \text{Tr}(X^\dagger Y)$ the Hilbert–Schmidt inner product.

The cardinality of $\underline{\rho}$ is not necessarily equal to that of $V(\mathcal{G})$, e.g. the same state can be associated to all vertices by the labeling $\ell(v) = \rho$, $\forall v \in V(\mathcal{G})$. Each vertex labeling ℓ is isomorphic to a tuple $(\ell(v))_{v \in V(\mathcal{G})} \in \mathcal{D}(\mathcal{H})^{|V(\mathcal{G})|}$. Given some $\underline{\rho}$ -labeling ℓ , we can see r as a function that outputs a tuple of two-state overlaps $r_\ell(\underline{\rho})$ for an input set $\underline{\rho}$. For instance, take $\underline{\rho} = \{|\psi\rangle\langle\psi|\} \cup \{\sigma_1, \sigma_2\}$ and $\ell(v) = |\psi\rangle\langle\psi|$ for all $v \in V(\mathcal{G})$, as above. Since all vertices of $V(\mathcal{G})$ have been assigned the same state, the associated $r_\ell(\underline{\rho})$ is $r_\ell(\underline{\rho}) = (1, 1, \dots, 1)$. When it is clear from the context which labeling ℓ is being used, we simply write $r(\underline{\rho})$.

Recall that, any edge-weight $r : E(\mathcal{G}) \rightarrow [0, 1]$ for an event graph \mathcal{G} , is said to have a quantum realization [45, 77] if there exists $\rho = \{\rho_i\}_{i \in V(\mathcal{G})}$ such that $r = r(\rho) \equiv (\text{Tr}(\rho_i \rho_j))_{\{i, j\} \in E(\mathcal{G})}$. We denote $|X|$ the cardinality of a set X . We say that a quantum state $\rho \in \mathcal{D}(\mathcal{H})$ is *pure* when $\text{Tr}(\rho^2) = 1$, in which case we denote it as a rank-1 projector $\rho = |\psi\rangle\langle\psi| \equiv \psi$.

Lemma 5. *Let $h : \mathbb{R}^{|E(\mathcal{G})|} \rightarrow \mathbb{R}$ be any convex-linear functional, acting over elements $r \in [0, 1]^{|E(\mathcal{G})|}$, for any event graph \mathcal{G} . Then, for any quantum realization $r = r(\underline{\rho})$ with states $\{\rho_i\}_i$, there exists a pure state quantum realization $r = r(\underline{\psi})$ with states $\{|\psi_i\rangle\}_i$, such that*

$$h(r(\underline{\rho})) \leq h(r(\underline{\psi})).$$

Moreover, $\underline{\psi} \subseteq \text{CONVHULL}(\underline{\rho})$.

Proof. Each $\rho_i \in \underline{\rho}$ is a convex combination of pure states $\{\psi_{\omega_i}^{(i)}\}_{\omega_i \in \Omega_i}$ for some set of pure states Ω_i . Noticing that $h(r)$ are, by construction, linear functionals over the overlaps,

$$\begin{aligned} \forall i, \rho_i &= \sum_{\omega} \lambda_{\omega}^{(i)} |\psi_{\omega}^{(i)}\rangle\langle\psi_{\omega}^{(i)}| \implies h(r(\{\rho_i\}_i)) \\ &= \sum_{\omega_1, \dots, \omega_m} \lambda_{\omega_1}^{(1)} \dots \lambda_{\omega_m}^{(m)} h\left(r\left(\left\{ \psi_{\omega_i}^{(i)} \right\}_i\right)\right). \end{aligned}$$

To conclude the above, one needs to introduce some redundant values of $1 = \sum_{\omega_i} \lambda_{\omega_i}^{(i)}$. The equation then follows from linearity with respect to r , and hence multilinearity with respect to the states.

We can collectively write $s = (\omega_1, \dots, \omega_m)$ and define $q_s = \lambda_{\omega_1}^{(1)} \dots \lambda_{\omega_m}^{(m)}$. Because each set of weights $\{\lambda_{\omega_i}^{(i)}\}_{\omega_i \in \Omega_i}$ correspond to convex weights, i.e. $\sum_{\omega_i} \lambda_{\omega_i}^{(i)} = 1$ with $0 \leq \lambda_{\omega_i} \leq 1$, we get that $\{q_s\}_s$ is also a set of convex weights. With this simplified notation we have that

¹⁷ Sometimes the inner-product $\langle \phi_i | \phi_j \rangle$ is called an overlap. We will not use this terminology here and simply refer to the overlap as the absolute value square of inner-product between states, or more generally, to the trace between the product of two density matrices.

$h(r(\{\rho_i\}_i)) = \sum_s q_s h(r(\{\psi_s^{(i)}\}_i))$ with $\sum_s q_s = 1$ and $0 \leq q_s \leq 1$. In other words, the linear functional h realized by overlaps between general quantum states can be written as the convex combination of the same functional realized by overlaps between pure states. Choosing now a particular s^* such that $\forall s, h(r(\{\psi_s^{(i)}\}_i)) \geq h(r(\{\psi_{s^*}^{(i)}\}_i))$ we see that

$$h(r(\{\rho_i\}_i)) = \sum_s q_s h\left(r\left(\left\{\psi_s^{(i)}\right\}_i\right)\right) \leq \sum_s q_s h\left(r\left(\left\{\psi_{s^*}^{(i)}\right\}_i\right)\right).$$

Since $\sum_s q_s = 1$ we have that $h(r(\{\rho_i\}_i)) \leq h(r(\{\psi_{s^*}^{(i)}\}_i))$. \square

Theorem 6. Let $h(r)$ be any linear-functional over $r = (r_e)_{e \in E(\mathcal{G})}$ for any event graph \mathcal{G} and $\mathfrak{Q}(\mathcal{G})$, defined by

$$\mathfrak{Q}(\mathcal{G}) := \{r : E(\mathcal{G}) \rightarrow [0, 1] : \exists \underline{\rho}, r = r(\underline{\rho})\},$$

be the set of quantum realizable edge-weights. Then, there always exists a pure state quantum realization $r = r(\underline{\psi})$ such that

$$h(r(\underline{\psi})) = \max_{r \in \mathfrak{Q}(\mathcal{G})} h(r).$$

The same holds if we restrict realizations to some convex and compact subset $\mathfrak{S} \subseteq \mathcal{D}(\mathcal{H})$ of all states, so that the quantum realizations are such that $r = r(\underline{\rho}_{\mathfrak{S}})$, with $\underline{\rho}_{\mathfrak{S}} \subseteq \mathfrak{S}$.

Proof. For any such h , lemma 5 shows that to every quantum realization $r = r(\underline{\rho})$, there exists a larger pure state realization within the convex hull of $\underline{\rho}$. Therefore, the maximum attainable value, among all quantum realizations $r \in \mathfrak{Q}(\mathcal{G})$, must be pure-state realizable, otherwise this would contradict lemma 5. The argument is the same if \mathfrak{S} is used instead. \square

This theorem implies the immediate corollary.

Corollary 1. The maximal quantum violation of any facet-defining inequality of $\mathfrak{C}(\mathcal{G})$, for any event graph \mathcal{G} , is attained by pure states.

Proof. Since $\mathfrak{C}(\mathcal{G})$ is a convex polytope, any facet-defining inequality from $\mathfrak{C}(\mathcal{G})$ is described by convex-linear functionals $h(r)$, together with some $b \in \mathbb{R}$ satisfying $h(r) \leq b$. \square

This corollary proves (and generalizes) a conjecture from [31], that the maximal bounds violating the $c_3(r) \leq 1$ inequality using pure states were also valid for mixed states in general and for any dimension. While here we will use these results to prove theorem 2, they are important by themselves for the event-graph approach and the theory of coherence witnesses.

Proof of theorem 2 of the main text. Due to theorem 6, we can restrict ourselves to pure stabilizer states. Consider first the 3-cycle inequality. We have

$$r_{1,2} + r_{1,3} - r_{2,3} \leq 1.$$

From theorem 1, we see that if all states in the graph are oblique to their neighbors there can be no violation since $r_{1,2} + r_{1,3} - r_{2,3} \leq r_{1,2} + r_{1,3} \leq \frac{1}{2^k} + \frac{1}{2^{k'}} \leq 1$ for all $k, k' = 1, \dots, n$. The same holds if we allow some edge-weights to be zero. If we allow any edge-weight in the inequality to be equal to one, it is simple to see that we cannot have a violation, as we would

have two nodes corresponding to the same stabilizer state, implying that the remaining pair of overlaps is equal. This shows the result for $c_3(r)$.

To show that the same is true for any m -cycle inequality we proceed by induction. Assume that an m -cycle inequality *cannot* be violated by quantum realizations $r = r(\rho_{\text{STAB}})$, with $\rho_{\text{STAB}} \subseteq \text{STAB}$. For any $(m+1)$ -cycle inequality we have that, $\forall e \in E(\mathcal{C}_{m+1})$,

$$-r_e + \sum_{\substack{e' \in E(\mathcal{C}_{m+1}) \\ e' \neq e}} r_{e'} \leq \sum_{\substack{e' \in E(\mathcal{C}_{m+1}) \\ e' \neq e}} r_{e'} \leq \frac{m}{2}$$

for any set of pure stabilizer states oblique or orthogonal to their neighbors in the graph. Since $m/2 \leq m-2$ for all $m \geq 4$ it remains to show that if two (or more) neighboring stabilizer states are equal we still cannot have a violation.

From lemma 4, if any edge-weight is equal to one, this implies that the cycle inequality from $\mathfrak{C}(\mathcal{C}_{m+1})$ becomes an inequality from $\mathfrak{C}(\mathcal{C}_m)$, which, by hypothesis, cannot be violated with the stabilizer subtheory, i.e. by any quantum realization $r = r(\rho_{\text{STAB}})$. We conclude that if the stabilizer subtheory cannot violate inequalities from $\mathfrak{C}(\mathcal{C}_m)$ it will also not violate the inequalities from $\mathfrak{C}(\mathcal{C}_{m+1})$. As we know this is true for the cycle inequalities $\mathfrak{C}(\mathcal{C}_3)$, by induction, this property must be satisfied by all facet-defining inequalities for the event graph polytopes $\mathfrak{C}(\mathcal{C}_m)$ for any m . \square

Appendix D. Proof of theorem 3

In this section, we start by building a series of results that are used to facilitate the proof of theorem 3.

The inequality $h_4(r) \leq 1$ is facet-defining for $\mathfrak{C}(\mathcal{K}_4)$, where \mathcal{K}_4 is the complete graph of four vertices. This inequality is given by

$$h_4(r) = r_{1,2} + r_{1,3} + r_{1,4} - r_{2,3} - r_{2,4} - r_{3,4} \leq 1. \quad (\text{D1})$$

We now demonstrate the following lemma.

Lemma 7. *Let $\mathcal{G} = \mathcal{K}_m$. If $r = r(\psi)$ such that the ψ -labeling $\ell: V(\mathcal{G}) \rightarrow \psi$ assigns the same pure state to adjacent vertices (any pair of vertices sharing an edge), then $\overline{h}_m(r(\psi)) \leq 1$.*

Proof. Without loss of generality, we may consider $r_{1,k^*} = 1$ for some $k^* \neq 1$. Let $r = r(\psi)$ be any pure state realization satisfying this constraint. In this case, we must have that $|\psi_1\rangle = |\psi_{k^*}\rangle$. Therefore, $r_{1,k} = r_{k^*,k}$ for all $k = \{2, \dots, m\} \setminus \{k^*\}$. The inequality $h_m(r) \leq 1$ is then written as

$$\begin{aligned}
h_m(r) &= \sum_{k=2}^m r_{1,k} - \sum_{i=2}^{m-1} \sum_{j>i}^m r_{i,j} \\
&= 1 + \sum_{\substack{k=2 \\ k \neq k^*}}^m r_{k^*,k} - \sum_{i=2}^{m-1} \sum_{\substack{j>i \\ j \neq k^*}}^m r_{i,j} \\
&= 1 - \sum_{\substack{i=2 \\ i \neq k^*}}^{m-1} \left(\sum_{\substack{j>i \\ j \neq k^*}}^m r_{i,j} \right) \leq 1
\end{aligned}$$

where we have used the fact that every element $r_{k^*,k}$ is present in the sum $\sum_{i=2}^{m-1} \sum_{j>i}^m r_{i,j}$. \square

Recall that $\mathfrak{Q}(\mathcal{G})$ is the set of all quantum realizable edge-weights given an event graph \mathcal{G} . Any stabilizer realization is (evidently) a quantum realization. In the remainder of this section, we will focus on situations concerning stabilizer realizations.

Consider a triple of non-orthogonal stabilizer states. We can use the value of two of the overlaps to lower bound the third.

Proposition 2. *Take three (arbitrary, non-orthogonal) n -qubit stabilizer states $|\psi_1\rangle$, $|\psi_2\rangle$, and $|\psi_3\rangle$ such that $r_{1,2} = 1/2^{N_2}$, $r_{1,3} = 1/2^{N_3}$ and $r_{2,3} \neq 0$. Then, $r_{2,3} \geq 1/2^{N_2+N_3}$ where $N_2, N_3 \in \{0, \dots, n\}$.*

Proof. Without loss of generality, we can take $|\psi_1\rangle = |0^n\rangle$. Let us start by considering the case where both $N_2, N_3 \neq 0$ or, equivalently, where $r_{1,2}, r_{1,3} \neq 1$. Since $r_{1,2} = 1/2^{N_2}$, we have that $|\psi_2\rangle$ is of the form

$$|\psi_2\rangle = \frac{1}{2^{N_2/2}} \left(|0^n\rangle + \sum_{j=1}^{2^{N_2}-1} i^{\alpha_j} |a_j\rangle \right)$$

where $\alpha_j \in \mathbb{Z}_4$ and $a_j \in \mathbb{F}_2^n \setminus \{0^n\}$. Similarly, $r_{1,3} = 1/2^{N_3}$ implies that the state $|\psi_3\rangle$ is of the form

$$|\psi_3\rangle = \frac{1}{2^{N_3/2}} \left(|0^n\rangle + \sum_{j=1}^{2^{N_3}-1} i^{\beta_j} |b_j\rangle \right),$$

where $\beta_j \in \mathbb{Z}_4$ and $b_j \in \mathbb{F}_2^n \setminus \{0^n\}$. From this, we see that

$$r_{2,3} = \frac{1}{2^{N_2+N_3}} \left| 1 + \sum_{j,j'} i^{\alpha_j - \beta_{j'}} \langle b_{j'} | a_j \rangle \right|^2.$$

If $r_{2,3} \neq 0$, it is clear from the expression above that $r_{2,3} \geq 1/(2^{N_2+N_3})$.

Finally, we note that, if either $N_i = 0$, we have the corresponding state $|\psi_i\rangle = |0^n\rangle$. In that case, it is clear that $r_{2,3} = 1/2^{N_j}$, with $j \neq i$, which complies with the lower bound established above. \square

Next, we demonstrate a result concerning realizations containing orthogonal states. This is the most important stepping stone to the proof of theorem 3 because realizations involving null edge-weights are significantly harder to analyze with respect to inequality violations.

Lemma 8. *Let $\mathcal{G} = \mathcal{K}_4$ and consider a quantum realization $r = r(\rho_{\text{STAB}}) \in \mathfrak{Q}(\mathcal{K}_4)$, where STAB denotes the set of n -qubit stabilizer states. If such a realization assigns to any two vertices two orthogonal states, then $h_4(r) \leq 1$.*

Proof. Consider the set of four (pure) n -qubit stabilizer states: $\{|\psi_1\rangle, |\psi_2\rangle, |\psi_3\rangle, |\psi_4\rangle\}$, where $|\psi_i\rangle$ is the stabilizer state associated with the i th vertex. The following observations follow trivially from lemma 7 when considering realizations with stabilizer states: (i) If four or more overlaps are zero, equation (D1) cannot be violated; (ii) If $|\psi_1\rangle$ is orthogonal to any of the other states, again no violation of equation (D1) is possible; (iii) To achieve a violation, at least two of the overlaps $r_{1,j}$ must equal $1/2$ and the remaining overlap with positive contribution must obey $r_{1,k} > r_{2,3} + r_{2,4} + r_{3,4}$ with $k \neq j$.

Throughout, we take $r_{1,2} = 1/2$ and $|\psi_2\rangle = |0^n\rangle$ which imposes that $|\psi_1\rangle = (|0^n\rangle + i^\alpha|s\rangle)/\sqrt{2}$, where $\alpha \in \mathbb{Z}_4$, $s \in \mathbb{F}_2^n \setminus \{0^n\}$, and $|s\rangle$ denotes the corresponding computational-basis state. Moreover, we can set $\alpha = 0$ because there is always a Clifford unitary that transforms $(|0^n\rangle + i^\alpha|s\rangle)/\sqrt{2}$ into $(|0^n\rangle + |s\rangle)/\sqrt{2}$ while leaving the state $|0^n\rangle$ unchanged. Thus, for simplicity, we take $|\psi_1\rangle = (|0^n\rangle + |s\rangle)/\sqrt{2}$. All of this is done w.l.o.g.

If we have three overlaps equal to zero, the only way for a violation to occur is that: (i) $r_{2,3} = r_{2,4} = r_{3,4} = 0$, (ii) $r_{1,3} = 1/2$, and (iii) $r_{1,4} > 0$. Note that the roles of $r_{1,3}$ and $r_{1,4}$ could be switched, leading exactly to the same conclusion. We will now show that these three conditions are incompatible. A generic stabilizer state takes the form:

$$|\psi_j\rangle = \frac{1}{\sqrt{|\mathcal{W}_j|}} \sum_{w \in \mathcal{W}_j} i^{\alpha_w} |w\rangle \quad (\text{D2})$$

where $\mathcal{W}_j \subseteq \mathbb{F}_2^n$ and $|\mathcal{W}_j| = 2^{N_j}$, for some $N_j \in \{0, n\}$. For the state to be a stabilizer state, \mathcal{W}_j and α_w must possess specific properties; these are irrelevant for the purposes of our proof and we will therefore omit them, but the interested reader is pointed to appendix A of [93] or theorem 9 of [41] for details.

Since, $r_{2,3} = 0$, for the state $|\psi_3\rangle$, 0^n cannot belong to \mathcal{W}_3 . Combining this observation with condition (ii) and given that $|\psi_1\rangle = (|0^n\rangle + |s\rangle)/\sqrt{2}$, it is clear that $|\psi_3\rangle = |s\rangle$. Because $r_{2,4} = r_{3,4} = 0$, the remaining state $|\psi_4\rangle$ must be a linear combination of computational-basis states so that $0^n, s \notin \mathcal{W}_4$. This necessarily means that $r_{1,4} = 0$, violating condition (iii).

If exactly two of the overlaps $\{r_{2,3}, r_{2,4}, r_{3,4}\}$ are zero, figure 6(a) illustrates the nine possible combinations of edge-weight assignments that could potentially lead to violations. Fortunately, symmetry constraints illustrated therein mean that we can restrict ourselves to only two different sub-cases.

Sub-case 1.—We consider the case depicted in the second row of the second column of figure 6(a): $r_{1,2} = r_{1,3} = 1/2$ and $r_{2,3} = r_{2,4} = 0$. Every scenario in the top two rows is equivalent to this one.

For a violation to occur, we must have $r_{1,4} > r_{3,4}$. The fact that $r_{1,3} = 1/2$ and $r_{2,3} = 0$ implies that $|\psi_3\rangle = |s\rangle$. The state placed at the fourth vertex can admit the form in equation (D2). Because $r_{2,4} = 0$ then $0^n \notin \mathcal{W}_4$; contrarily, since $r_{3,4} \neq 0$, $s \in \mathcal{W}_4$. Immediately, this means that $r_{1,4} = 1/2^{N_4+1}$ while $r_{3,4} = 1/2^{N_4}$, which means that $r_{3,4} > r_{1,4}$, and therefore no violation can occur.

Sub-case 2.—We now consider the sub-cases in the bottom row of figure 6(a) which are all equivalent between themselves, but non-equivalent to the six sub-cases in the top two rows.

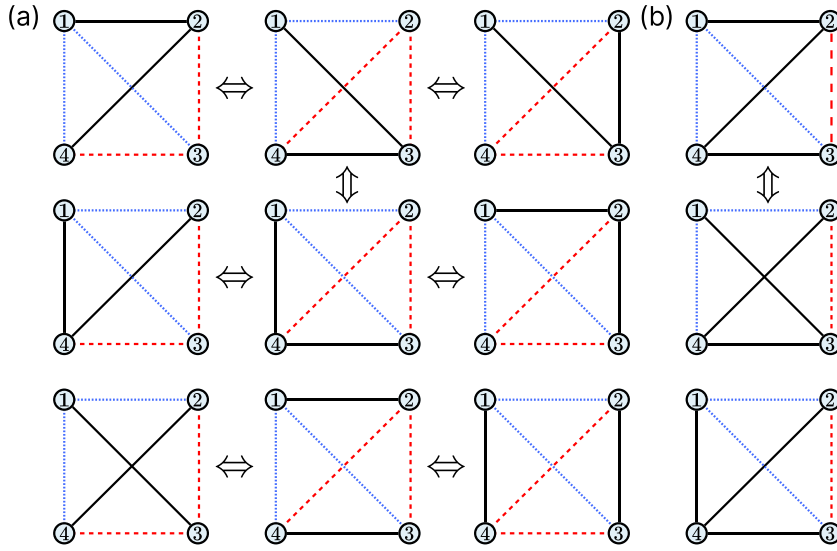


Figure 6. Vertex assignments with null edge-weights. The figure illustrates the cases where (a) exactly two overlaps are zero and (b) there is exactly one null overlap. Dashed-red lines indicate edges of the graph with an assigned weight equal to zero, dotted-blue lines represent the edges assigned with the value $1/2$, while solid-black lines depict edges with positive (but arbitrary) edge-weight.

We take the edge-weight assignment on the first column: $r_{1,2} = r_{1,4} = 1/2$ and $r_{2,3} = r_{3,4} = 0$. This means that, for a violation to occur $r_{1,3} > r_{2,4}$. The condition that $r_{1,4} = 1/2$ enforces one of the following three forms for $|\psi_4\rangle$:

$$|\psi_4\rangle = \begin{cases} |0^n\rangle \\ |s\rangle \\ \frac{|0^n\rangle + i^\beta |s\rangle}{\sqrt{2}}, \beta \in \{1, 3\} \end{cases}.$$

Lemma 7 informs us that the first option will lead to no violation; moreover, the second option leads to $r_{2,4} = 0$ taking us back to the three-null-overlaps situation which we already proved leads to no violation. This leaves us with the last option, that is: $|\psi_4\rangle = (|0^n\rangle + i^\beta |s\rangle)/\sqrt{2}$, with $\beta \in \{1, 3\}$. Immediately, we see that $r_{2,4} = 1/2$, and therefore it is impossible to meet that condition that $r_{1,3} > r_{2,4}$, so that no violation is possible in this case either.

Finally, it remains to assess the case where only a single null overlap exists. Figure 6(b) illustrates the three possible edge-weight assignments that may lead to violations. We note that the top two scenarios are equivalent, meaning that, again, we have to focus only on two subcases.

Sub-case 1.—We consider $r_{1,2} = r_{1,4} = 1/2$ and $r_{2,3} = 0$ (second row of figure 6(b)). For a violation to occur, the following must hold $r_{1,3} > r_{2,4} + r_{3,4}$. We note that $r_{1,4} = 1/2$ and $r_{2,4} \neq 0$ implies that $|\psi_4\rangle = (|0\rangle + i^\beta |s\rangle)/\sqrt{2}$, with $\beta = \{1, 3\}$. This fixes $r_{2,4} = 1/2$ which immediately means that the condition $r_{1,3} > r_{2,4} + r_{3,4}$ can never be met, and therefore no violation can occur.

Sub-case 2.—We consider $r_{1,2} = r_{1,3} = 1/2$ and $r_{2,3} = 0$. This means that for a violation to hold, we must have $r_{1,4} > r_{2,4} + r_{3,4}$. The fact that $r_{1,3} = 1/2$ and $r_{2,3} = 0$ implies that $|\psi_3\rangle = |s\rangle$. The state in the fourth vertex can assume the general form given by equation (D2) where

both 0^n and s must belong to the set \mathcal{W}_4 (otherwise, we fall back into the cases with two or three null overlaps). Automatically this means that $r_{2,4} = r_{3,4} = 1/2^{N_4}$. On the other hand, $r_{1,4}$ can be (at most) $r_{1,4} = 1/2^{N_4-1}$, which means that the condition $r_{1,4} > r_{2,4} + r_{3,4}$ cannot be met, and therefore no violation can occur.

This concludes the assessment of all possible cases. Therefore, if any overlap $r_{i,j}$ is zero, no violation of the inequality (D1) is possible. \square

Finally, we have all the tools needed to prove theorem 3.

Proof of theorem 3 of the main text. Consider a set of four (pure) n -qubit stabilizer states: $\{|\psi_1\rangle, |\psi_2\rangle, |\psi_3\rangle, |\psi_4\rangle\}$. Recall that, if we want to find a violation of equation (D1), no two states can be the same (lemma 7) so that: $|\psi_i\rangle \neq |\psi_j\rangle$ for $i \neq j$. Therefore, to obtain $h_4 > 1$ the following conditions must hold: (i) there are at least two $r_{1,j} = 1/2$, (ii) the remaining overlap $r_{1,k}$ with $k \neq j$ must obey: $r_{1,k} > r_{2,3} + r_{2,4} + r_{3,4}$.

Without loss of generality, take $|\psi_1\rangle = |0^n\rangle$ and assume that $r_{1,2} = r_{1,4} = 1/2$. Under these assumptions, for a violation to occur we must have $r_{1,3} > r_{2,3} + r_{2,4} + r_{3,4}$.

Because $r_{1,2} = 1/2$ this means that $|\psi_2\rangle = (|0^n\rangle + |s\rangle)/\sqrt{2}$ where $s \in \mathbb{F}_2^n \setminus \{0^n\}$. Evidently, something similar can be said for $|\psi_4\rangle$: $|\psi_4\rangle = (|0^n\rangle + i^\alpha |w\rangle)/\sqrt{2}$, with $w \in \mathbb{F}_2^n \setminus \{0^n\}$ and $\alpha \in \mathbb{Z}_4$. This will impose a constraint on the overlap $r_{2,4}$:

$$r_{2,4} = \begin{cases} 1, & \text{if } w = s \wedge \alpha = 0 \\ 0, & \text{if } w = s \wedge \alpha = 2 \\ 1/2, & \text{if } w = s \wedge \alpha = \{1, 3\} \\ 1/4, & \text{if } w \neq s \end{cases} \quad (\text{D3})$$

Lemmas 7 and 8 guarantee, respectively, that the first and second options give no violation and we can thus focus on the other two.

Taking $r_{2,4} = 1/2$ we have: $r_{1,3} > 1/2 + r_{2,3} + r_{3,4}$, which is impossible to verify since at most $r_{1,3}$ can be $1/2$.

Taking $r_{2,4} = 1/4$ we get the condition $r_{1,3} > 1/4 + r_{2,3} + r_{3,4}$. In order for this to hold, $r_{1,3}$ must be equal to $1/2$ which implies that the corresponding state must take the form $|\psi_3\rangle = (|0^n\rangle + i^\beta |t\rangle)/\sqrt{2}$. Immediately, this will imply that the values for $r_{2,3}$ and $r_{3,4}$ are bounded as $r_{2,4}$ in equation (D3). Since we know realizations with null overlaps to yield no violation (lemma 8), it is clear that the condition $r_{1,3} > 1/4 + r_{2,3} + r_{3,4}$ can never be met, because $r_{1,3}$ can be at most $1/2$.

Theorem 6 guarantees that this holds also for mixed stabilizer states. This concludes the proof. \square

We conclude this section by generalizing theorem 3 for d -dimensional qudits.

Theorem 9. *There exists no quantum realization $r = r(\rho_{\text{STAB}(d)}) \in \mathfrak{Q}(\mathcal{K}_4)$, where $\text{STAB}(d)$ denotes the set of stabilizer states of n d -dimensional qudits, such that $h_4(r) > 1$, for any integer value $n \geq 1$.*

Proof. The overlap $|\langle\psi|\phi\rangle|^2$ of any two non-orthogonal stabilizer states, $|\psi\rangle$ and $|\phi\rangle$, of n qudits of dimension d can assume value $1/d^N$ with $0 \leq N \leq n$, see lemma 2 of [94] on the overlap between pure stabilizer states.

Again, lemma 7 guarantees that, if any state is repeated, there is no violation of the inequality, so we assume all states to be different. The positive terms in $h_4(r)$ lead to $r_{1,2} + r_{1,3} + r_{1,4} = 3/d$, in the best case. For $d = 3$ this leads to a value of at most 1 and for $d > 3$ the value will

be smaller than one. As a consequence, it is immediately realized that no violation of the inequality is possible. \square

References

- [1] Eisert J, Hangleiter D, Walk N, Roth I, Markham D, Parekh R, Chabaud U and Kashefi E 2020 Quantum certification and benchmarking *Nat. Rev. Phys.* **2** 382–90
- [2] Streltsov A, Adesso G and Plenio M B 2017 Colloquium: quantum coherence as a resource *Rev. Mod. Phys.* **89** 041003
- [3] Baumgratz T, Cramer M and Plenio M B 2014 Quantifying coherence *Phys. Rev. Lett.* **113** 140401
- [4] Horodecki R, Horodecki P, Horodecki M and Horodecki K 2009 Quantum entanglement *Rev. Mod. Phys.* **81** 865–942
- [5] Erhard M, Krenn M and Zeilinger A 2020 Advances in high-dimensional quantum entanglement *Nat. Rev. Phys.* **2** 365–81
- [6] Brunner N, Pironio S, Acin A, Gisin N, Méthot A A and Scarani V 2008 Testing the dimension of Hilbert spaces *Phys. Rev. Lett.* **100** 210503
- [7] Budroni C, Cabello A, Gühne O, Kleinmann M and Larsson J-A 2022 Kochen-specker contextuality *Rev. Mod. Phys.* **94** 045007
- [8] Preskill J 2018 Quantum Computing in the NISQ era and beyond *Quantum* **2** 79
- [9] Cai Z, Babbush R, Benjamin S C, Endo S, Huggins W J, Li Y, McClean J R and O’Brien T E 2023 Quantum error mitigation *Rev. Mod. Phys.* **95** 045005
- [10] Bharti K et al 2022 Noisy intermediate-scale quantum algorithms *Rev. Mod. Phys.* **94** 015004
- [11] Bravyi S and Kitaev A 2005 universal quantum computation with ideal clifford gates and noisy ancillas *Phys. Rev. A* **71** 022316
- [12] Gottesman D 1997 Stabilizer codes and quantum error correction *PhD Dissertation* Caltech
- [13] Zhou X, Leung D W and Chuang I L 2000 Methodology for quantum logic gate construction *Phys. Rev. A* **62** 052316
- [14] Litinski D and v. Oppen F 2018 Lattice surgery with a twist: simplifying clifford gates of surface codes *Quantum* **2** 62
- [15] Litinski D 2019 Magic state distillation: not as costly as you think *Quantum* **3** 205
- [16] Litinski D 2019 A game of surface codes: large-scale quantum computing with lattice surgery *Quantum* **3** 128
- [17] Gidney C and Fowler A G 2019 Efficient magic state factories with a catalyzed $|CCZ\rangle$ to $2|T\rangle$ transformation *Quantum* **3** 135
- [18] Broadbent A and Schaffner C 2015 Quantum cryptography beyond quantum key distribution *Des. Codes Cryptogr.* **78** 351–82
- [19] Chitambar E and Gour G 2019 Quantum resource theories *Rev. Mod. Phys.* **91** 025001
- [20] Campbell E T 2011 Catalysis and activation of magic states in fault-tolerant architectures *Phys. Rev. A* **83** 032317
- [21] Haug T and Kim M 2023 Scalable measures of magic resource for quantum computers *PRX Quantum* **4** 010301
- [22] Gross D, Nezami S and Walter M 2021 Schur–Weyl duality for the Clifford group with applications: property testing, a Robust Hudson theorem and de Finetti representations *Commun. Math. Phys.* **385** 1325–93
- [23] Haug T, Lee S and Kim M S 2024 Efficient quantum algorithms for stabilizer entropies *Phys. Rev. Lett.* **132** 240602
- [24] Tirrito E, Tarabunga P S, Lami G, Chanda T, Leone L, Oliviero S F E, Dalmonte M, Collura M and Hamma A 2024 Quantifying nonstabilizerness through entanglement spectrum flatness *Phys. Rev. A* **109** L040401
- [25] Turkschi X, Schirò M and Sierant P 2023 Measuring nonstabilizerness via multifractal flatness *Phys. Rev. A* **108** 042408
- [26] Liu Z-W and Winter A 2022 Many-body quantum magic *PRX Quantum* **3** 020333
- [27] Bravyi S, Browne D, Calpin P, Campbell E, Gosset D and Howard M 2019 Simulation of quantum circuits by low-rank stabilizer decompositions *Quantum* **3** 181
- [28] Bravyi S and Gosset D 2016 Improved classical simulation of quantum circuits dominated by Clifford gates *Phys. Rev. Lett.* **116** 250501

[29] Bravyi S, Smith G and Smolin J A 2016 Trading classical and quantum computational resources *Phys. Rev. X* **6** 021043

[30] Veitch V, Mousavian S A H, Gottesman D and Emerson J 2014 The resource theory of stabilizer quantum computation *New J. Phys.* **16** 013009

[31] Galvão E F and Brod D J 2020 Quantum and classical bounds for two-state overlaps *Phys. Rev. A* **101** 062110

[32] Wagner R, Barbosa R S and Galvão E F 2024 Inequalities witnessing coherence, nonlocality and contextuality *Phys. Rev. A* **109** 032220

[33] Designolle S, Uola R, Luoma K and Brunner N 2021 Set coherence: basis-independent quantification of quantum coherence *Phys. Rev. Lett.* **126** 220404

[34] Salazar R, Czartowski J and de Oliveira Junior A 2022 Resource theory of absolute negativity (arXiv:2205.13480 [quant-ph])

[35] Buscemi F, Chitambar E and Zhou W 2020 Complete resource theory of quantum incompatibility as quantum programmability *Phys. Rev. Lett.* **124** 120401

[36] Martins E, Savi M F and Angelo R M 2020 Quantum incompatibility of a physical context *Phys. Rev. A* **102** 050201

[37] Uola R, Kraft T, Shang J, Yu X-D and Gühne O 2019 Quantifying quantum resources with conic programming *Phys. Rev. Lett.* **122** 130404

[38] Ducuara A F, Lipka-Bartosik P and Skrzypczyk P 2020 Multiobject operational tasks for convex quantum resource theories of state-measurement pairs *Phys. Rev. Res.* **2** 033374

[39] Wagner R, Schwartzman-Nowik Z, Paiva I L, Te’eni A, Ruiz-Molero A, Barbosa R S, Cohen E and Galvão E F 2024 Quantum circuits for measuring weak values, Kirkwood-Dirac quasiprobability distributions and state spectra *Quantum Sci. Technol.* **9** 015030

[40] Fernandes C, Wagner R, Novo L and Galvão E F 2024 Unitary-invariant witnesses of quantum imaginarity *Phys. Rev. Lett.* **133** 190201

[41] García H J, Markov I L and Cross A W 2014 On the geometry of stabilizer states *Quantum Inf. Comput.* **14** 683–720

[42] Giordani T, Esposito C, Hoch F, Carvacho G, Brod D J, Galvão E F, Spagnolo N and Sciarrino F 2021 Witnesses of coherence and dimension from multiphoton indistinguishability tests *Phys. Rev. Res.* **3** 023031

[43] Brod D J, Galvão E F, Viggianiello N, Flamini F, Spagnolo N and Sciarrino F 2019 Witnessing genuine multiphoton indistinguishability *Phys. Rev. Lett.* **122** 063602

[44] Giordani T, Brod D J, Esposito C, Viggianiello N, Romano M, Flamini F, Carvacho G, Spagnolo N, Galvão E F and Sciarrino F 2020 Experimental quantification of four-photon indistinguishability *New J. Phys.* **22** 043001

[45] Thomas F 2023 An estimation theoretic approach to quantum realizability problems *PhD Dissertation*

[46] Napoli C, Bromley T R, Cianciaruso M, Piani M, Johnston N and Adesso G 2016 Robustness of coherence: an operational and observable measure of quantum coherence *Phys. Rev. Lett.* **116** 150502

[47] Wu K, Strelets A, Regula B, Xiang G, Li C and Guo G 2021 Experimental progress on quantum coherence: detection, quantification and manipulation *Adv. Quantum Technol.* **4** 2100040

[48] Silva M, Faleiro R, Mateus P and Cruzeiro E Z 2023 A coherence-witnessing game and applications to semi-device-independent quantum key distribution *Quantum* **7** 1090

[49] Ma Z-H, Cui J, Cao Z, Fei S-M, Vedral V, Byrnes T and Radhakrishnan C 2019 Operational advantage of basis-independent quantum coherence *Europhys. Lett.* **125** 50005

[50] Radhakrishnan C, Ding Z, Shi F, Du J and Byrnes T 2019 Basis-independent quantum coherence and its distribution *Ann. Phys., NY* **409** 167906

[51] Yao Y, Dong G H, Xiao X and Sun C P 2016 Frobenius-norm-based measures of quantum coherence and asymmetry *Sci. Rep.* **6** 32010

[52] Giordani T et al 2023 Experimental certification of contextuality, coherence and dimension in a programmable universal photonic processor *Sci. Adv.* **9** eadj4249

[53] Pauwels J, Pironio S and Tavakoli A 2024 Information capacity of quantum communication under natural physical assumptions (arXiv:2405.07231 [quant-ph])

[54] Tavakoli A, Cruzeiro E Z, Woodhead E and Pironio S 2022 Informationally restricted correlations: a general framework for classical and quantum systems *Quantum* **6** 620

[55] Miklin N and Oszmaniec M 2021 A universal scheme for robust self-testing in the prepare-and-measure scenario *Quantum* **5** 424

[56] Flammia S T, Gross D, Liu Y-K and Eisert J 2012 Quantum tomography via compressed sensing: error bounds, sample complexity and efficient estimators *New J. Phys.* **14** 095022

[57] Yuen H 2023 An improved sample complexity lower bound for (fidelity) quantum state tomography *Quantum* **7** 890

[58] Haah J, Harrow A W, Ji Z, Wu X and Yu N 2016 Sample-optimal tomography of quantum states *Proc. 48th Annual ACM Symp. on Theory of Computing (STOC'16. ACM)*

[59] O'Donnell R and Wright J 2016 Efficient quantum tomography *Proc. 48th Annual ACM Symp. on Theory of Computing (STOC'16. ACM)*

[60] Chen S, Huang B, Li J, Liu A and Sellke M 2023 When does adaptivity help for quantum state learning? *2023 IEEE 64th Annual Symp. on Foundations of Computer Science (FOCS)* (IEEE) pp 391–404

[61] Buhrman H, Cleve R, Watrous J and de Wolf R 2001 Quantum fingerprinting *Phys. Rev. Lett.* **87** 167902

[62] Hong C K, Ou Z Y and Mandel L 1987 Measurement of subpicosecond time intervals between two photons by interference *Phys. Rev. Lett.* **59** 2044–6

[63] Shchesnovich V S and Bezerra M E O 2018 Collective phases of identical particles interfering on linear multiports *Phys. Rev. A* **98** 033805

[64] Fanizza M, Rosati M, Skotiniotis M, Calsamiglia J and Giovannetti V 2020 Beyond the swap test: optimal estimation of quantum state overlap *Phys. Rev. Lett.* **124** 060503

[65] Quek Y, Kaur E and Wilde M M 2024 Multivariate trace estimation in constant quantum depth *Quantum* **8** 1220

[66] Oszmaniec M, Brod D J and Galvão E F 2024 Measuring relational information between quantum states and applications *New J. Phys.* **26** 013053

[67] Beverland M, Campbell E, Howard M and Kliuchnikov V 2020 Lower bounds on the non-clifford resources for quantum computations *Quantum Sci. Technol.* **5** 035009

[68] Pashayan H, Wallman J J and Bartlett S D 2015 Estimating outcome probabilities of quantum circuits using quasiprobabilities *Phys. Rev. Lett.* **115** 070501

[69] Seddon J R, Regula B, Pashayan H, Ouyang Y and Campbell E T 2021 Quantifying quantum speedups: Improved classical simulation from tighter magic monotones *PRX Quantum* **2** 010345

[70] Heimendahl A, Montealegre-Mora F, Vallentin F and Gross D 2021 Stabilizer extent is not multiplicative *Quantum* **5** 400

[71] Jiang J and Wang X 2023 Lower bound for the t count via unitary stabilizer nullity *Phys. Rev. Appl.* **19** 034052

[72] Rall P, Liang D, Cook J and Kretschmer W 2019 Simulation of qubit quantum circuits via Pauli propagation *Phys. Rev. A* **99** 062337

[73] Leone L, Oliviero S F E and Hamma A 2022 Stabilizer Rényi entropy *Phys. Rev. Lett.* **128** 050402

[74] Haug T and Piroli L 2023 Stabilizer entropies and nonstabilizerness monotones *Quantum* **7** 1092

[75] Oliviero S F E, Leone L, Hamma A and Lloyd S 2022 Measuring magic on a quantum processor *njp Quantum Inf.* **8** 148

[76] Bluvstein D et al 2023 Logical quantum processor based on reconfigurable atom arrays *Nature* **626** 58–65

[77] Wagner R, Camillini A and Galvão E F 2024 Coherence and contextuality in a Mach-Zehnder interferometer *Quantum* **8** 1240

[78] Pont M et al 2022 Quantifying n -photon indistinguishability with a cyclic integrated interferometer *Phys. Rev. X* **12** 031033

[79] Masot-Llima S and Garcia-Saez A 2024 Stabilizer tensor networks: universal quantum simulator on a basis of stabilizer states (arXiv:2403.08724 [quant-ph])

[80] Cusumano S, Venuti L C, Cepollaro S, Esposito G, Iannotti D, Jasser B, Odaivć J, Viscardi M and Hamma A 2025 Non-stabilizerness and violations of chsh inequalities (arXiv:2504.03351[quant-ph])

[81] Macedo R A, Andriolo P, Zamora S, Poderini D and Chaves R 2025 Witnessing magic with bell inequalities (arXiv:2503.18734[quant-ph])

[82] Howard M, Wallman J, Veitch V and Emerson J 2014 Contextuality supplies the ‘magic’ for quantum computation *Nature* **510** 351–5

- [83] Schmid D, Du H, Selby J H and Pusey M F 2022 Uniqueness of noncontextual models for stabilizer subtheories *Phys. Rev. Lett.* **129** 120403
- [84] Lillystone P, Wallman J J and Emerson J 2019 Contextuality and the single-qubit stabilizer subtheory *Phys. Rev. Lett.* **122** 140405
- [85] Spekkens R W 2005 Contextuality for preparations, transformations and unsharp measurements *Phys. Rev. A* **71** 052108
- [86] Cabello A, Severini S and Winter A 2014 Graph-theoretic approach to quantum correlations *Phys. Rev. Lett.* **112** 040401
- [87] Amaral B and Cunha M T 2018 *On Graph Approaches to Contextuality and Their Role in Quantum Theory* (*Springer Briefs in Mathematics*) (Springer)
- [88] Shrikhande S S 1959 The uniqueness of the L_2 association scheme *Ann. Math. Stat.* **30** 781–98
- [89] Bharti K, Ray M, Xu Z-P, Hayashi M, Kwek L-C and Cabello A 2022 Graph-theoretic approach for self-testing in bell scenarios *PRX Quantum* **3** 030344
- [90] Mermin N D 1990 Extreme quantum entanglement in a superposition of macroscopically distinct states *Phys. Rev. Lett.* **65** 1838–40
- [91] Tavakoli A, Pozas-Kerstjens A, Brown P and Araújo M 2024 Semidefinite programming relaxations for quantum correlations *Rev. Mod. Phys.* **96** 045006
- [92] Navascués M and Vértesi T 2015 Bounding the set of finite dimensional quantum correlations *Phys. Rev. Lett.* **115** 020501
- [93] Nest M V D 2010 Classical simulation of quantum computation, the Gottesman-Knill theorem and slightly beyond *Quantum Inf. Comput.* **10** 258–71
- [94] Kueng R and Gross D 2015 Qubit stabilizer states are complex projective 3-designs (arXiv:1510.02767)